JOM

Structure and Properties of Al–0.6%Zr–0.4%Fe–0.4%Si (wt%) Wire Alloy Manufactured by Electromagnetic Casting

--Manuscript Draft--

Manuscript Number:	JOMJ-D-19-00943R1
Full Title:	Structure and Properties of Al–0.6%Zr–0.4%Fe–0.4%Si (wt%) Wire Alloy Manufactured by Electromagnetic Casting
Article Type:	Original Paper
Corresponding Author:	Torgom Akopyan, Dr National University of Science and Technology MISiS RUSSIAN FEDERATION
Corresponding Author Secondary Information:	
Corresponding Author's Institution:	National University of Science and Technology MISiS
Corresponding Author's Secondary Institution:	
First Author:	Nikolay Belov, Dr.
First Author Secondary Information:	
Order of Authors:	Nikolay Belov, Dr.
	Natalia Korotkova
	Torgom Akopyan, Dr
	Viktor Timofeev
Order of Authors Secondary Information:	
Funding Information:	Government of the Russian Federation (074-02-2018-329) — Not applicable
Abstract:	The experimental Al–0.6%Zr–0.4%Fe–0.4%Si alloy has been manufactured by using the method of electromagnetic casting (EMC). It is shown that Zr is completely dissolved in the aluminum solid solution (Al) and iron is fully included in the Al8Fe2Si phase. The fine microstructure of the as-cast rod implies a high deformation plasticity, which has been experimentally confirmed during wire production. The cold rolled wire has UTS ~ 260 MPa and subsequent annealing at 400 °C for 3 h. slightly reduces the strength which is associated with the stabilizing effect of the L12 (Al3Zr) phase nanoparticles formed during annealing. Annealing also leads to a significant increase in the specific conductivity, the value of which reaches 57.0 IACS. Drawing of the annealed rolled wire leads to significant strengthening. Annealing at 400 0C leads to a marked strength reduction, which, however, remains high enough for conductive alloys (UTS higher than 200 MPa).
Response to Reviewers:	We thank the reviewer for constructive comments, which helped us to improve the manuscript. Below, we address all comments point-by-point, discussing the subsequent modifications. On behalf of all co-authors, Dr. Akopyan T.K. Reviewer #1: Question 1): 1. Introduction, Line 8, more information is needed on the "Properzi" and "Southwire" mills? are they trademarks? Answer: Yes, they are. Corresponding information is added.

Question 2): - are the elemental percentages in wt.%?

Answer: Yes. The corresponding information is added into the «Experimental» section.

Question 3): at what scale is the EMC-casting trials performed?

Answer: EMC-casting is an industrial technology that allows obtaining rods with a diameter of 12 or 8 mm and a length of up to 20 m. For the current studies, a rod with a diameter of 8 mm and a length of 20 m was obtained by using this industrial facility. For laboratory rolling, a 0.5 m long sample was cut from this EMC rod. Corresponding clarifications are added into the «Experimental» section.

Question 4): - what was the shape of the ingot? how were the samples cut from that? what are the details of rolling?

Answer: The ingot for the rolling is a rod with a diameter of 8 mm and a length of ~0.5 m which was cut from the initial EMC rod with a length of ~20 m. Corresponding clarifications are added into the «Experimental» section.

Question 5): - did the ingots receive any homogenization treatment after casting and prior to rolling? if yes, please bring the details.

Answer: As indicated in the «Experimental» section, wire with a square cross-section of 1x1 mm was obtained at room temperature from the as-cast EMC rod (the reduction ratio was 98 %). Thus, the rolling of the ingot was carried out without preliminary annealing or heating. Corresponding clarifications are added into the «Experimental» section.

Question 6): - you need a diagram to demonstrate the thermomechanical routing

Answer: We agree with the recommendation. The diagram is added into the supplementary materials.

Question 7): - What does EMS stand for (line 50)?

Answer: EMS is a misprint. EMS is everywhere changed to EMC (electromagnetic casting)

Question 8): - There are no chemical compositions on Table 1

Answer: We agree with the comment. Improper description of Table 1 is deleted.

Question 9): - In Table 1, what are the annealing times?

Answer: The annealing time is 3 h. The corresponding information is added in the Table 1.

Question 10): - Table 1, to anneal a sample at a certain temperature, you take a sample from a lower class annealing temperature?

Answer: Yes, to anneal a sample at a higher temperature, we take a sample from a lower annealing temperature. The annealing mod is additionally demonstrated in the diagram in the supplementary materials.

Question 11): - What is the melting point of the alloy?

Answer: As indicated in section 3.1 (second paragraph), the solidus temperature is

631 °C.

Question 12): - Fig. 1b and 1c, the horizontal axes must be the mass fraction of solid rather than Zr

Answer: We agree with the comment. Corresponding correction was made to Fig. 1b and 1c

Question 13): - section 3.3, line 20, …, which can be attributed to the formation of recrystallized grains [6]. and coarsening of particles? if not, mention why?

Answer: We agree with the comment. Corresponding correction was made to the text: «…which can be attributed to coarsening of the Al3Zr precipitates and formation of recrystallized grains.»

Question 14): - section 3.3, line 32, … the decomposition rate of Al is higher than for the EMC rod. Why?

Answer: Due to the increased density of defects in the crystal lattice, the decomposition rate of (Al) in the strip is higher than that for the as-cast EMC rod. Corresponding clarification is added to the text.

Question 15): - section 3.3, line 39, the decrease of EC at higher temperatures can be accounted for by an increase in the solubility of Zr in Al. Please bring a citation.

Answer: We agree with the comment. Corresponding reference is added to the text.

Question 16): - section 3.3, line 43, Fig. 4 requires more description than this.

Answer: We agree with the comment. The description of this part is expanded.

Question 17): - Fig.3, you have performed at least 5 indentations per point. Why don't you report the error bars?

Answer: We agree with the comment. The error bars are added.

Question 18): - section 3.4, line 50, you do not bring any other specimen from another casting method to prove that the EMC posses the favorable microstructure. considering the fact that the objective of your work is to show how EMC leads to an improvement of electrical conductivity, you need to make a comparison with other casting techniques (e.g. DC).

Answer: We agree with the comment. The microstructure of the alloy obtained at a solidification rate close to industrial (~10 K/s) is added in Fig. 5c. According to the presented data, the alloy structure contains an unacceptable primary Al3Zr phase crystals.

Question 19): - line 47, sediment instead of concentrated.

Answer: We agree with the comment. Corresponding correction was made to the text.

Question 20): - what does CCR stand for?

Answer: As indicated in the Introduction, CCR is «continuous casting and rolling».

Question 21): - equation (1) requires citation

Answer: Equation (1) is a personal development of the authors of this article and it is mentioned for the first time.

	Question 22): - the paragraph before the last one, "the concentration of Si in Al can be reduced by increasing the iron content in the alloy. In particular..." this paragraph requires revision, it sounds very vague. Answer: We agree with the comment. The paragraph is revised. It is added clarification that «The concentration of Si in (Al) can be reduced by increasing the iron content due to the formation of the Al8Fe2Si compound». Question 23): Summary (Conclusions?) - number 6 is very ambiguous. Answer: We agree with the comment. Summary is changed to Conclusions. Conclusion number 6 is deleted.

Dear Editor,

We thank for the constructive comments, which helped us to improve the manuscript. In file labeled "Response to Reviewers" we point-by-point respond to all the issues rose in the comments of the reviewer. The main changes in the text of the article are highlighted in green.

On behalf of all co-authors,

Dr. Akopyan T.K.

Structure and Properties of Al–0.6%Zr–0.4%Fe–0.4%Si (wt%) Wire Alloy Manufactured by Electromagnetic Casting

Nikolay A. Belov[1], Natalia O. Korotkova[1], Torgom K. Akopyan[1,2], Viktor N.Timofeev[3]

[1]National University of Science and Technology MISiS, 4 Leninsky pr., Moscow, 119049, Russia

[2]Baikov Institute of Metallurgy and Materials Science, 49 Leninsky pr., Moscow, 119991, Russia

[3]Siberian Federal University, 79 Svobodnyy prospekt., Krasnoyarsk, 660041, Russia

Abstract

The experimental Al–0.6%Zr–0.4%Fe–0.4%Si alloy has been manufactured by using the method of electromagnetic casting (EMC). It is shown that Zr is completely dissolved in the aluminum solid solution (Al) and iron is fully included in the Al_8Fe_2Si phase. The fine microstructure of the as-cast rod implies a high deformation plasticity, which has been experimentally confirmed during wire production. The cold rolled wire has UTS ~ 260 MPa and subsequent annealing at 400 °C for 3 h. slightly reduces the strength which is associated with the stabilizing effect of the $L1_2$ (Al_3Zr) phase nanoparticles formed during annealing. Annealing also leads to a significant increase in the specific conductivity, the value of which reaches 57.0 IACS. Drawing of the annealed rolled wire leads to significant strengthening. Annealing at 400 ^{0}C leads to a marked strength reduction, which, however, remains high enough for conductive alloys (UTS higher than 200 MPa).

Keywords: Aluminum-zirconium alloys; electrical conductivity, electromagnetic casting, phase composition, mechanical properties

Corresponding author: Torgom Akopyan **Email:** nemiroffandtor@yandex.ru

1. Introduction

Aluminum alloys of the Al–Zr system are widely used in thermally stable cable products that should combine high electrical conductivity and sufficient strength preserved after heating to ~300 °C [1-3]. Wire rods for electrical cables are typically manufactured by using of a complex of continuous casting and rolling (CCR). The most popular companies providing such equipment are well known “Continuus-Properzi” [4] and “Southwire” [5]. The desired characteristics of Al-Zr wire (first of all, electrical conductivity, strength and thermal stability) depend considerably on the processing parameters of wire rods, which includes zirconium concentration, casting conditions, rolling regime and, most importantly, the heat treatment cycle [6]. According to the experimental results for the conductivity of alloys containing 0.2–0.3% Zr (hereinafter wt.% unless otherwise stated) the peak values occur after annealing at 350–400 °C for hundreds of hours [7, 8]. Optimization of the CCR process is a difficult task due to its complexity compared to conventional processing which is characterized by time and space separated processes used for ingot production and subsequent deformation.

Positive influence of zirconium on the thermal stability is caused by nanoparticles of the $L1_2$ (Al_3Zr) phase formed in wire rods as a result of the decomposition of a supersaturated aluminum solid solution (hereinafter (Al)) during annealing [9-15]. As shown earlier [9], these nanoparticles start to precipitate at between 350 and 375 °C, achieving peak hardening at 400–450 °C. It was shown [6] that an increase in the zirconium content from 0.2 to 0.5 % leads to a significant increase in the thermal stability without a decrease in the electrical conductivity. Since zirconium sharply increases the liquidus temperature, the melting and casting temperatures of those alloys should be significantly higher compared to conventional ones, which is not always achievable in industrial production, including the CCR technology.

In our opinion, a promising technology for the production of conductive aluminum alloys with a high concentration of zirconium (more than 0.5%) is the method of electromagnetic casting (EMC) which allows producing long ingots with small cross section [16,17]. The EMC technology provides casting at a sufficiently high temperature (up to 900 °C) and ultra-high solidification rates (10^3 –10^4 K/s). This allows achieving the same structure as in the alloys produced with the RS / PM technology (rapid solidification / powder metallurgy) [18-20]. The good promise of the EMC method has been demonstrated for the production of conductive aluminum alloys containing about 7% RE [21] which were previously developed specifically for RS / PM technology [18].

Some strengthening of aluminum alloys without a significant reduction in their electrical conductivity can be achieved by adding iron in an amount of up to 1%, which is implemented in

a number of branded alloys (for example, 8076). In terms of the best plasticity, (this is important for providing the necessary manufacturability during drawing), the most favorable morphology among the iron phases has the Al_8Fe_2Si phase, the formation of which requires a certain amount of silicon [22-24]. The presence of iron and silicon in alloy is also advisable from the viewpoint of cost reduction since these elements are the main impurities in commercial aluminum. Silicon is usually an undesirable impurity in the conductive alloys, however, according to some data, this element accelerates the precipitation of the Zr-containing phase during annealing [25-27].

Thus, based on the above, the aim of this work was to substantiate the promise of the EMC method for producing conductor alloys based on the Al – Zr – Fe – Si system containing at least 0.5% Zr.

2. Experimental methods

The chemical composition of the experimental alloy obtained by the EMC (Oxford Instruments) method was the Al–0.62%Zr–0.41%Fe–0.39%Si (throughout the article, the content of elements is indicated in wt.% (unless otherwise specified)). The equipment of Research and Production Centre of Magnetic Hydrodynamics was used [28]. The melting was carried out in an induction furnace in a graphite-chased crucible based on commercial aluminum (99.5 wt.%). Zr, Fe and Si were introduced into the aluminum melt in the form of master alloys (Al-5%Zr, 80%Fe-20%flux and Al–12%Si) at ~850 °C. The casting was carried out by the EMC method at a temperature of ~830 °C in order to obtain the long-length cast rod with a diameter of 8 mm and a length of ~20 m. For laboratory rolling, a 0.5 m long sample was cut from the EMC rod.

By using laboratory rolls of VEM-3SM, wire with a square cross-section of 1x1 mm was obtained at room temperature from the as-cast EMC rod (the reduction ratio was 98 %). Thus, the rolling of the rod was carried out without preliminary annealing or heating of the ingot. From this wire, after intermediate annealing at 400 ^{0}C, wires with diameters of 0.5 mm and 0.26 mm were obtained by drawing (the reduction degrees were 80% and 95% respectively). The resulting wire was studied in the as-drawn state and after annealing at 400°C. The main stages of the processing route are summarized in Table 1. Additionally a 2 mm strip was obtained by cold rolling of the as-cast EMC billet for studying the effect of the annealing temperature on the hardness and electrical conductivity (EC). The diagram of the thermomechanical routings is presented in supplementary materials (refer to online supplementary material, Fig. S-1).

The microstructure was examined by means of scanning electron microscopy (SEM, TESCAN VEGA 3), electron microprobe analysis (EMPA, OXFORD AZtec) and transmission electron microscopy (TEM, JEM−2100). Polished samples were used for the studies. Mechanical

polishing was used, as well as electrolytic polishing, which was carried out at a voltage of 12 V in an electrolyte containing six parts C_2H_5OH, one part $HClO_4$ and one part glycerine. The thin foils for TEM were prepared by ion thinning with a PIPS (Precision Ion Polishing System, Gatan) machine and studied at 160 kV. Additionally the microstructure of the experimental alloy was examined after slow solidification (in the furnace) from 850 ^{0}C and after rapid solidification (in water) from 750 ^{0}C.

Table 1 Deforming and heating treatment of the experimental alloy

Designation	Regime
EMC rod (diameter 8 mm)	
R0	As-cast
R300	Annealing at 300 ^{0}C for 3 h
R350	R300 + annealing at 350 ^{0}C (3 h)
R400	R350 + annealing at 400 ^{0}C (3 h)
R450	R400 + annealing at 450 ^{0}C (3 h)
R500	R450 + annealing at 500 ^{0}C (3 h)
R550	R500 + annealing at 550 ^{0}C (3 h)
R600	R550 + annealing at 600 ^{0}C (3 h)
Cold rolled EMC rod to strip (thickness 2 mm)	
S0	Cold rolled strip
S300	Annealing at 300 ^{0}C for 3 h
S350	S300 + annealing at 350 ^{0}C (3 h)
S400	S350 + annealing at 400 ^{0}C (3 h)
S450	S400 + annealing at 450 ^{0}C (3 h)
S500	S450 + annealing at 500 ^{0}C (3 h)
S550	S500 + annealing at 550 ^{0}C (3 h)
S600	S550 + annealing at 600 ^{0}C (3 h)
Wires produced from as-cast EMC rod	
W1	Cold rolling of 8 mm rod to 1 mm wire (reduction 98%)
W1-400	Annealing of 1 mm wire at 400 ^{0}C during 3 hours
W0.5	Drawing of 1mm wire (annealed at 400 ^{0}C) to 0.5 mm (reduction 80%)
W0.26	Drawing of 1mm wire (annealed at 400 ^{0}C) to 0.26 mm (reduction 95%)
W0.5-400	Annealing of 0.5 mm wire at 400 ^{0}C during 1 hours
W0.26-400	Annealing of 0.26 mm wire at 400 ^{0}C during 1 hours

Room-temperature tensile tests were conducted for as-processed bar specimens on a Zwick Z250 universal testing machine (the loading rate was 10 mm/min). The Vickers hardness (HV) was measured using a Metkon Duroline MH-6 universal tester with a load of 1 kg and a dwell time of 10 s. The hardness was measured at least five times at each point. The specific conductivity of the EMC rod and the cold rolled strip was determined using the eddy current method with a VE-26NP eddy structurescope.

The phase composition of the quaternary system Al–Zr–Fe–Si was calculated using Thermo-Calc software (TTAL5 database) [29].

3. Results

3.1. Calculation of phase composition

The element concentrations in the experimental alloy were chosen based on the following principles. According to [6,14,15,30], the concentration of zirconium corresponds to the maximum value up to which the precipitation hardening grows in an almost linear manner. The Fe and Si concentrations are close to their maximum contents in commercial aluminum and, as shown earlier [23], should ensure complete binding of iron into the Al_8Fe_2Si phase.

As can be seen from the vertical cross-section calculated at 0.4% Fe and 0.4% Si (Fig.1a), with an increase in the zirconium content the liquidus temperature rises sharply and reaches 822 °C at 0.6% Zr. This temperature corresponds to the onset of the formation of primary Al_3Zr phase crystals ($D0_{23}$), while the aluminum solid solution forms at a temperature below 660 °C. According to this cross-section, the Al_3Fe and Al_8Fe_2Si phases should also form during equilibrium solidification in addition to (Al) and Al_3Zr, the solidus temperature being 631 °C. The third iron-containing phase Al_5FeSi can only form in the solid state.

It is well-known that the non-equilibrium solidification of low-alloyed Al – Fe – Si system alloys significantly complicates their phase composition [23]. According to the calculation based on the Sheil-Gulliver model which allows one to evaluate the nature of solidification at low cooling rates, one can expect the formation of all the above mentioned iron-containing phases (see Fig.1b), as well as (Si). On the other hand, zirconium (in the amounts considered herein) at a high cooling rate can fully dissolve in (Al) [14]. There are also indications that an increased cooling rate suppresses the formation of Al_3Fe and Al_5FeSi phases in alloys containing iron and silicon at concentrations close to the selected ones [23]. Taking into account the analysis above, a corrected calculation of the non-equilibrium solidification was carried out (Fig.1c). The calculation suggests that after solidification of (Al) at 657 °C, the

Al_8Fe_2Si phase should form as part of a binary eutectic. Solidification should end at 576 °C via a eutectic reaction involving the (Si) phase, the amount of which, however, should be very small.

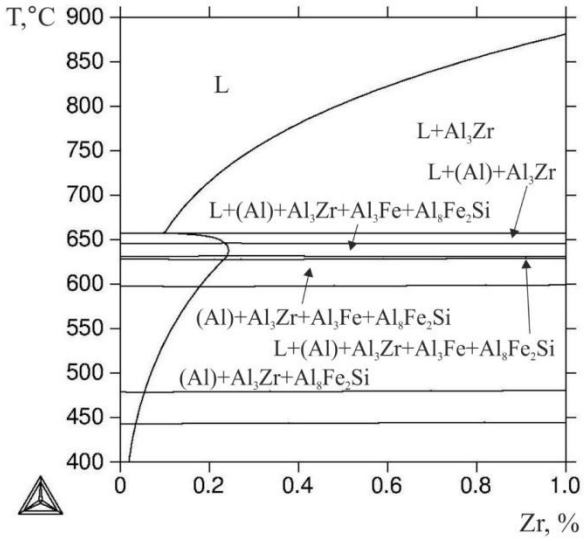

a

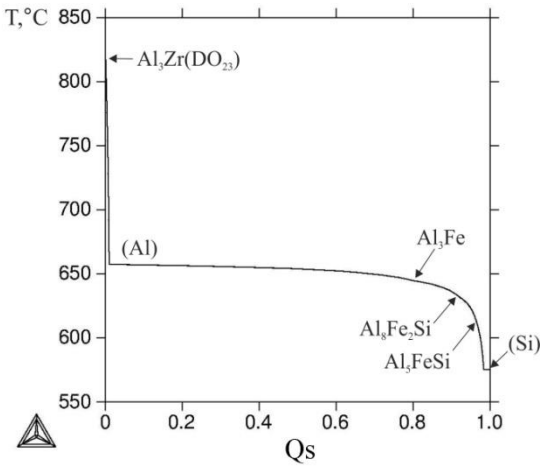

b

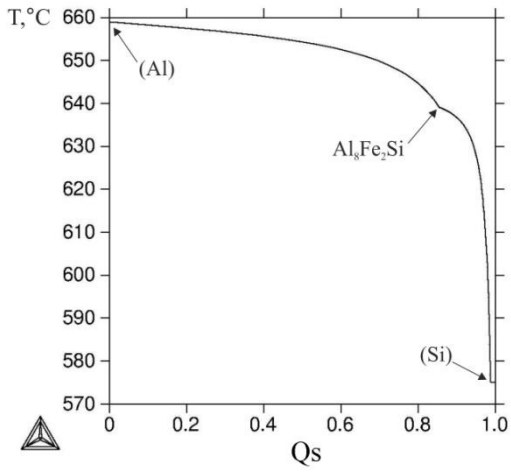

c

Figure 1. The isopleth of Al–Zr–Fe–Si phase diagram at 0.4%Fe and 0.4%Si (a) and mass fraction of solid phases (Qs) versus temperature (Sheil-Gulliver simulation) for alloy Al–0.6%Zr–0.4%Fe–0.4%Si (b,c): b) all phases are entered; c) phases Al_3Zr, Al_3Fe and Al_5FeSi are suspended (e.g. Zr in (Al))

3.2. Characterization of as-cast EMC rod

The microstructure of the as-cast billet appears to be fairly homogeneous and is characterized by a fine structure, which can be detected only by scanning electron microscopy (Fig.2a). Analysis of the microstructure did not reveal primary Al_3Zr phase crystals. This

indicates the complete dissolution of zirconium in the (Al) composition. The size of the dendritic cells is about 5 μm, which, according to [31], corresponds to a cooling rate of more than 10^3 K/s. The veins with a thickness of about 0.2 μm are revealed along the boundaries of the dendritic cells (Fig.2b). According to [32–34], such a structure is typical of the Al_8Fe_2Si phase in a small amount.

After annealing of the as-cast billet at up to 400 °C, no visible changes in the microstructure are observed. At higher temperatures, the morphology of the Fe-containing phase changes significantly. The formation of globular particles can be observed already at 450 °C (Fig.2c). It should be noted that among Fe-containing phases of the Al – Fe – Si system, only Al_8Fe_2Si is capable of spheroidization [23]. Subsequent heating to 550 °C slightly affects the microstructure (Fig.2d, e). At the maximum heating temperature (600 °C), the Fe-containing phase particles grow, the size of some particles reaching 1 μm (Fig.1f). EMPA analysis of these particles confirms their Al_8Fe_2Si composition. In addition, the particles with a size of about 0.1 μm (isolated fragment in Fig.1f), which can be interpreted as secondary precipitates of the Al_3Zr ($D0_{23}$) phase, are detected. As can be seen from the vertical cross-section shown in Fig.1a, the presence of these two phases corresponds to the equilibrium state of the considered alloy at 600 °C.

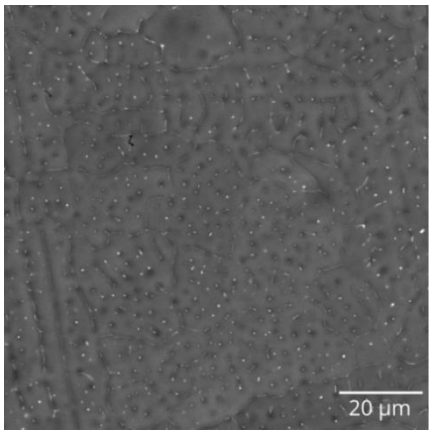

a

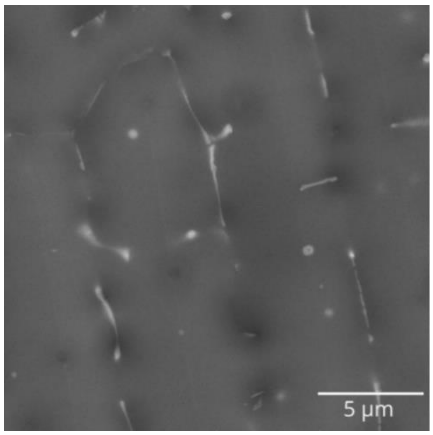

b

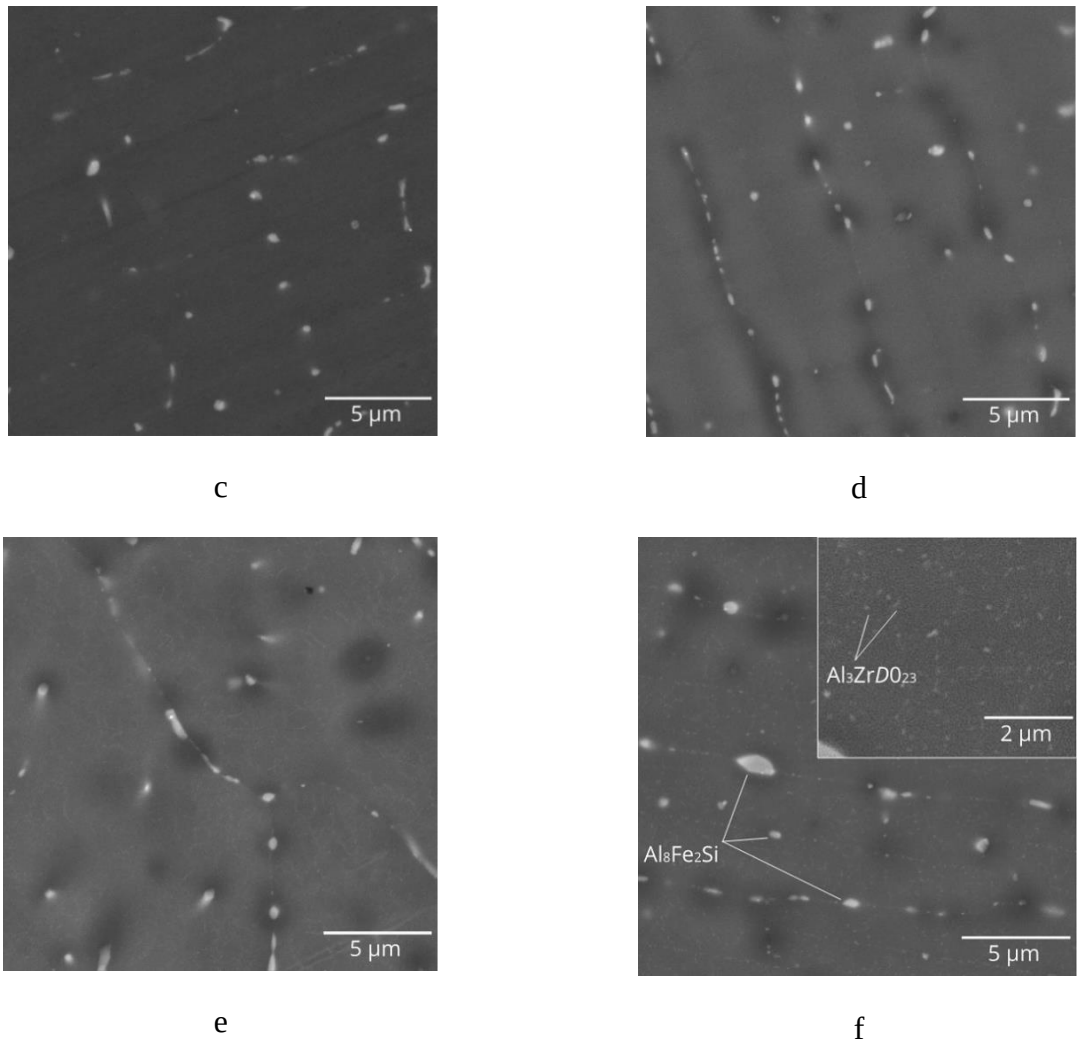

Figure 2. Effect of annealing temperature on microstructures of the Al–0.6%Zr–0.4%Fe–0.4%Si alloy, EMC rod, SEM: a,b) as-cast, c) R450, d) R500, e) R550, f) R600 (see in Table 1)

3.3. Effect of annealing and rolling on hardness and electrical conductivity

The high content of Zr in (Al) implies a significant precipitation hardening of the as-cast billet due to the formation of the $L1_2$ (Al_3Zr) phase nanoparticles. The dependence shown in Fig.3a shows that the maximum hardness which is twice the initial one (in the as-cast state) is achieved after heating at 400 °C. An increase of the annealing temperature to above 450 °C leads to softening which can be explained, primarily, by the enlargement of the Al_3Zr precipitates [9-12]. Rolling of the cylindrical billet to a 2 mm strip increases the hardness from 410 to 600 MPa, and its subsequent annealing leads to further hardening (Fig.3a). The maximal hardness of the cold rolled strip is somewhat smaller compared to that of the as-cast billet, which can be accounted for by the competition of two processes: hardening due to the formation of $L1_2$ (Al_3Zr) nanoparticles and softening due to the processes of recovery. Annealing of the strip at

higher temperatures leads to lower hardness compared to that of the EMC rod, which can be attributed to coarsening of the Al_3Zr precipitates and formation of recrystallized grains [6].

The formation of $L1_2$ (Al_3Zr) nanoparticles leads to a decrease in the Zr concentration in (Al) and, as a consequence, to an increase of the alloy electrical conductivity. The dependencies given in Fig.3b confirm this suggestion. The EC value increases from 23.8 to 31.6 MS/m for EMC rod and from 23.6 to 33.7 MS/m for cold rolled strip (i.e., by 33% and 41%, respectively). It should be noted that due to the increased density of defects in the crystal lattice, the decomposition rate of (Al) in the strip is higher [35] than that for the as-cast EMC rod. Indeed, in the former case, the maximum EC is reached after annealing at 550 ^{0}C, while in the latter case it is reached at 500 ^{0}C. In both cases, these values are higher than the maximum hardening temperature (Fig.3a). The decrease of EC at higher temperatures can be accounted for by an increase in the solubility of Zr in (Al) [6]. The EBSD analysis of the strip structure shows that the fibrous (non-recrystallized) structure formed during rolling is preserved in the as-annealed state for annealing at up to 400 °C (Fig.4a). It is clearly seen that the fibrous grains contain an extensive network of low angle boundaries. In accordance with TEM, the subgrains have an average size of about 1 μm (Fig.4b). TEM also reveals a large number of nanoparticles with a diameter of about 10 nm (Fig.4c). According to SADP (Fig.4d), these nanoparticles correspond to the $L1_2$ type phase precipitates.

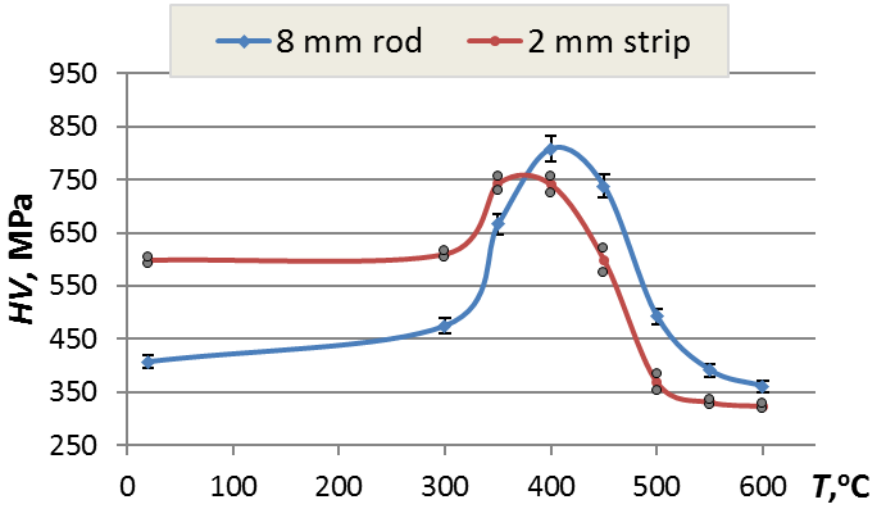

a

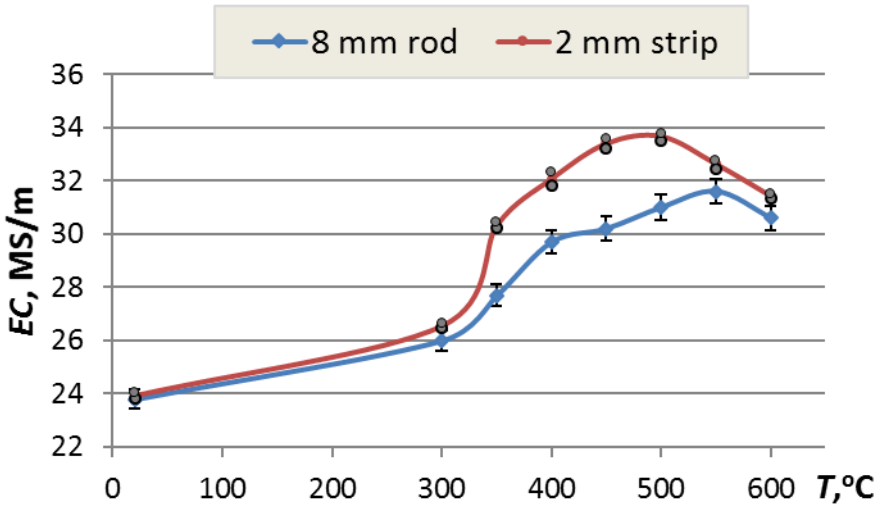

b

Fig. 3. Hardness (a) and electrical conductivity (b) vs. temperature curves for Al–0.6%Zr–0.4%Fe–0.4%Si alloy

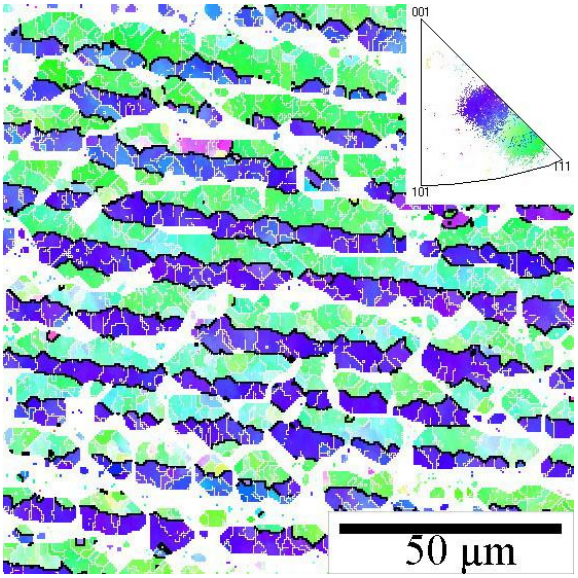

a

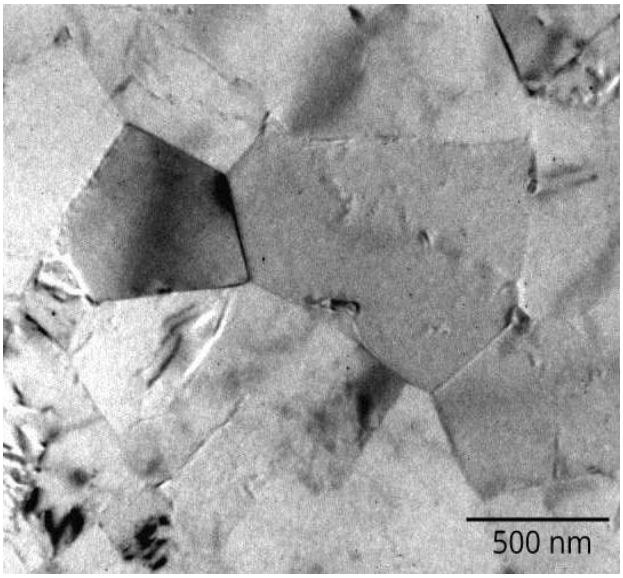

b

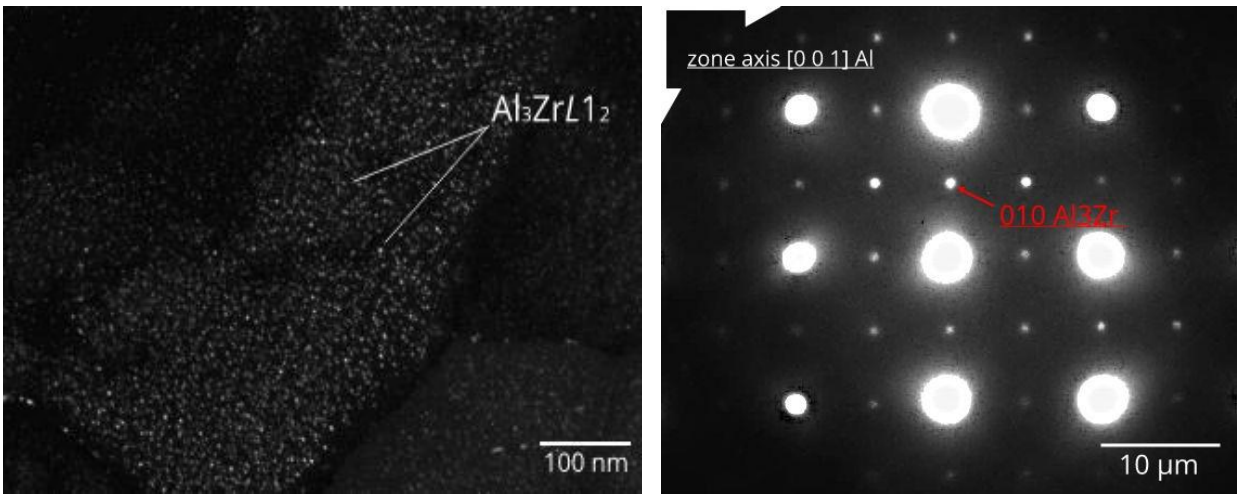

c d

Figure 4. EBSD (a) and TEM (b-d) structure of the alloy Al–0.6%Zr–0.4%Fe–0.4%Si after cold rolling and annealing at 400 ^{0}C (S400, see in Table 2): a) longitudinal direction, b) transverse direction (bright field). c) dark field, b) diffraction patterns

3.4. Properties of wire

The favorable microstructure of the as-cast EMC rod implies a high deformation plasticity, which has been experimentally confirmed during wire production using both cold rolling and drawing. As in the case of cold rolled strip, the main structural change was the formation of elongated grains, while the morphology of the Al_8Fe_2Si phase remained almost unchanged. The cold rolled wire has UTS ~ 260 MPa and YS ~ 230 MPa (zirconium must remain in (Al)). The results obtained for the strip, in particular, the temperature dependences of hardness and EC (Fig.3b) were used as the basis for choosing the annealing temperature of the wire, i.e., 400 °C. Annealing at this temperature (state W1-400) for 3 hours slightly reduced UTS and YS (Table 2). This result can be attributed to the stabilizing effect of the Al_3Zr nanoparticles. Drawing of the annealed rolled wire leads to significant strengthening. In particular, UTS are 270 MPa for the 0.5 mm wire and 300 MPa for the 0.26 mm wire. Annealing at 400 ^{0}C leads to a marked strength reduction, which, however, remains high enough for conductive alloys (UTS higher than 200 MPa).

Table 2 Mechanical properties of wires

State[1]	UTS, MPa	YS, MPa	El, %
W1	259 ± 5	233 ± 7	1.6 ± 0.4
W1-400	231 ± 4	212 ± 3	3.3 ± 0.5

W0.5	274 ± 3	259 ± 3	2.3 ± 0.2
W0.26	301 ± 5	284 ± 4	0.6 ± 0.2
W0.5-400	224 ± 6	199 ± 3	2.6 ± 0.6
W0.26-400	207 ± 3	181 ± 4	2.8 ± 0.4

[1] see in Table 2

4. Discussion

Summarizing the available information, we can conclude that the combination of strength, electrical conductivity and thermal stability in comparison with alloys containing about 0.3% Zr can be significantly improved by the addition of 0.6% Zr. This improvement can be accounted for by the formation of a favorable structure due to a combination of high solidification rate, high casting temperature, cold deformation of as-cast EMC rod and annealing of wire.

Slow cooling during solidification leads to the formation of primary Al_3Zr phase crystals ($D0_{23}$), which, due to their greater density, are sediment at the bottom of the ingot (Fig.5a). In addition, needle-shaped and skeletal particles whose compositions are Al_3Fe and Al_8Fe_2Si, respectively, are detected in the structure of the slowly cooled sample. These changes correspond to the simulation of non-equilibrium crystallization shown in Fig.1b. The microstructure of the sample obtained by water quenching of the initial billet after 1 hour exposure at 750^0C (i.e. melt production) also reveals the presence of the primary Al_3Zr phase crystals (Fig.5b). This is because this temperature is below the liquidus temperature of the alloy (see in Fig.1a). Thus the combination of high temperature of melt and rapid solidification achieved in the EMC method leads to the desired microstructure of the as-cast rod (Fig. 2a,b). For comparison, Fig. 1 shows the microstructure of the alloy obtained during solidification in a graphite mold (with a size of 10 x 40 x 200 mm). Due to the relatively low cooling rate (~10 K/s), which is typical of industrial production [23], the alloy structure contains a small amount of unacceptable primary Al_3Zr phase crystals.

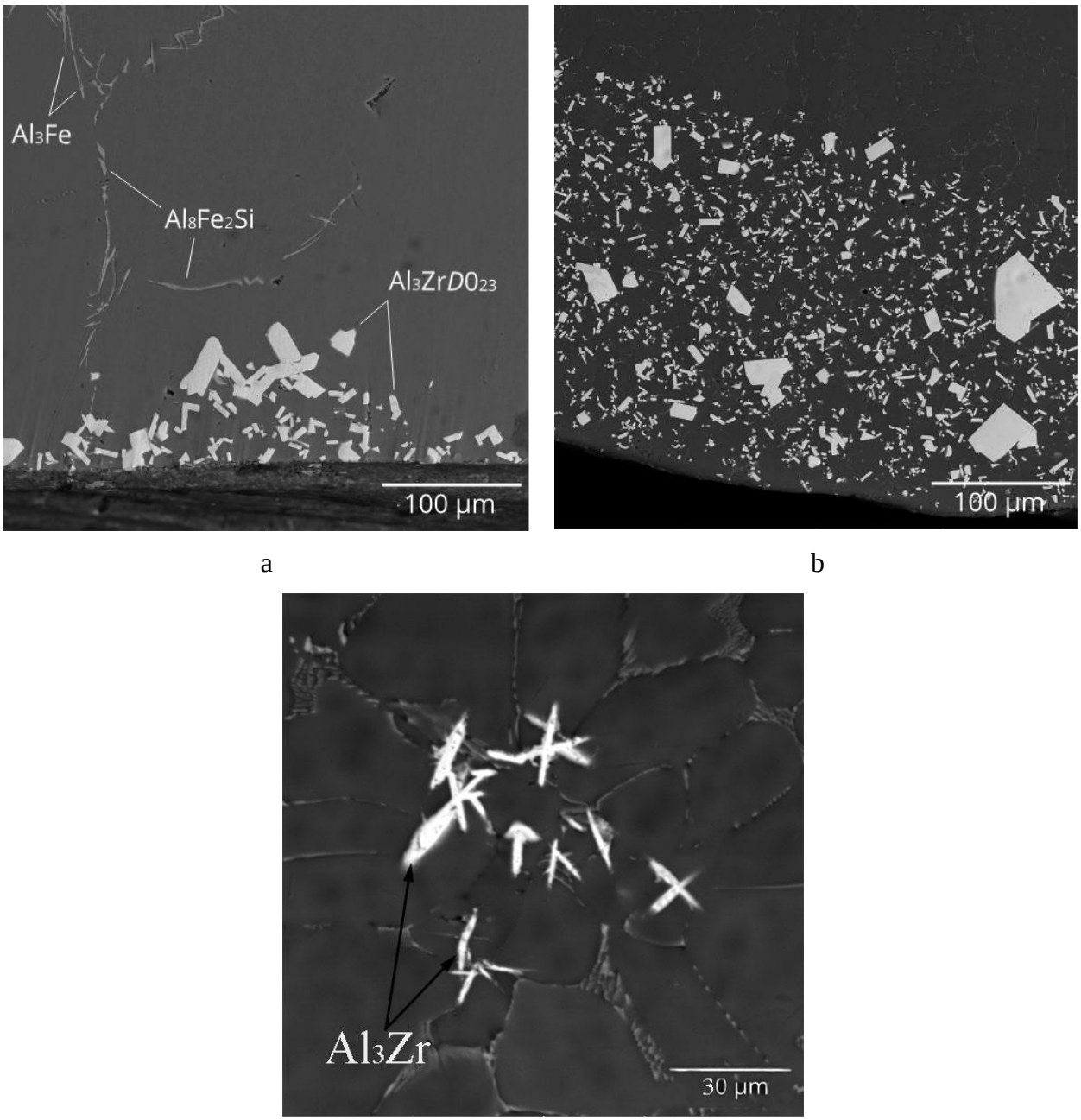

Figure 5. Microstructures of the alloy Al–0.6%Zr–0.4%Fe–0.4%Si after slow cooling from 850 ^{0}C (a), after quenching from 750 ^{0}C (b) and after solidification in a graphite mold (cooling rate is about 10 K/s). SEM:

The dependencies of the hardness versus annealing temperature shown in Fig.3a allow us to estimate the potential hardening and thermal stability. Since heating at 400 °C corresponds to the maximum hardness, it is obvious that the wire should be annealed at this temperature. Such annealing stabilizes the structure at the maximum operating temperatures of the conductor alloys (according to IEC 62004: 2007). Thus, unlike the CCR technology which includes continuous annealing of wire [7,8], the EMC technology provides a significant reduction of the production cycle.

The desired combination of strength, ductility and electrical conductivity (EC) can be achieved by selecting the chemical composition and annealing mode. Since any alloying that is required for achieving strength and, especially, thermal stability leads to a decrease in the electrical conductivity, it is advisable to estimate the maximum achievable EC. In the case of Al – Zr – Fe – Si alloys, the maximum EC level can be approximately calculated using the equation:

$$EC=(Q / 100) \cdot (EC_0 – C_{Zr} \cdot K_{Zr} – C_{Si} \cdot K_{Si}) \quad (1)$$

where Q is the fraction of (Al) (wt.%), EC_0 is the electrical conductivity of pure aluminum (MS/m), C_{Zr} and C_{Si} are the concentrations of Zr and Si in (Al) (wt.%), and K_{Zr} and K_{Si} are the coefficients of Zr and Si on EC (per 1 wt.%)

From earlier work [26] where the separate and joint influence of zirconium and silicon on the properties of pure aluminum was considered it follows that the coefficients K_{Zr} and K_{Si} are ~ 20 and ~ 10, respectively. To estimate EC using Eq. (1), it is also necessary to determine Q, C_{Zr} and C_{Si}. For this purpose, we calculated the phase composition of the alloy for the case of the iron is completely bound into the Al_8Fe_2Si phase. The calculated EC values were compared with experimental data for the strip (see in Fig.3b). As can be seen from Table 3, at 450 ^{0}C there is a good match between the calculated and the experimental values. This suggests that the proposed equation is adequate. On the other hand, at 400 ^{0}C the calculated EC is higher than the experimental one. This can be attributed to the fact that the annealing time was insufficient to achieve the equilibrium solubility of Zr in (Al). With decreasing temperature, the diffusion rate of zirconium in (Al) decreases and thus it requires longer exposures which can be hundreds of hours [7, 8]. Therefore, annealing the wire at temperatures below 400 °C seems impractical, despite the potential to achieve higher EC values.

Table 3 Calculated phase composition and electrical conductivity (EC) for some alloys of Al–Zr–Fe–Si system

T, ^{0}C	Fractions of phases, wt.%				Concentrations in (Al), wt.%			EC, MS/m (IACS)	
	Al_8Fe_2Si	(Si)	Al_3Zr	(Al)	Si	Fe	Zr	Calc	Exper
Al–0.6%Zr–0.4%Fe–0.4%Si									
400	1.23	0.04	1.10	97.64	0.26	<0.01	0.02	34.0 (58.6)	32.1 (55.3)
450	1.22	–	1.10	97.72	0.30	<0.01	0.04	33.2 (57.2)	33.4 (57.0)
Al–0.6%Zr–0.4%Fe–0.15%Si									

400	1.22	–	1.10	97.68	0.05	<0.01	0.02	36.0 (62.1)	–
Reference alloy Al–0.28%Zr–0.14%Fe–0.07%Si [6]									
400	0.41	–	0,46	99.13	0.02	<0.01	0.02	36.4 (62,8)	33.4 (57.6)
Al–0.6%Zr–1.2%Fe–0.4%Si									
400	3.68	–	1.10	95.22	0.09	<0.01	0.02	34.8 (60.0)	–

Since it is impossible to reduce the residual solubility of Zr in (Al), it is advisable to consider the possibility of reducing the concentration of Si in (Al) in order to increase the EC. As can be seen from Table 3, the reduction of silicon content in the alloy to 0.15 % makes it possible to reduce its concentration in (Al) to 0.05%, which implies an increase in EC up to 36.0 (almost to the level of the reference alloy Al – 0.28% Zr – 0.14% Fe– 0.07% Si). The concentration of Si in (Al) can be reduced by increasing the iron content due to the formation of the Al_8Fe_2Si compound. For instance, the addition of 0.8% Fe into the experimental alloy (i.e., up to 1.2%) according to the calculation suggests an increase in the EC from 34.0 to 34.8 MS/m, although the amount of the Al_8Fe_2Si phase increases by 3 times. This is due to the fact that the effect of reducing the concentration of Si in (Al) (from 0.26 to 0.09%) is more significant than the decrease of the fraction of (Al).

Thus, the use of the EMC technology for the Al-Zr-Fe-Si system alloys provides several advantages. First, this is an increase in the zirconium content in (Al) compared to the CCR technology, which allows increasing the strength and maximum operating temperature. Secondly, excluding the hot rolling operation from the wire production process simplifies the technology (up to combining continuous casting with drawing). Thirdly, the fine microstructure (submicron size of eutectic particles) allows increasing the permissible contents of iron and silicon, which implies economic advantages.

5. Conclusions

1. For the experimental Al – 0.6% Zr – 0.4% Fe – 0.4% Si alloy, it was shown that, due to the high cooling rate during solidification, the method of electromagnetic casting (EMC) shows good promise for obtaining wires with an improved combination of strength, electrical conductivity and thermal stability.

2. Using both experimental and computational methods, it was shown that in order to ensure complete dissolution of zirconium into an aluminum solid solution, the casting temperature should be above 820 ° C.

3. The iron in the as-cast billet is fully included in the Al_8Fe_2Si phase, which has the form of veinlets located along the boundaries of the dendritic cells. Annealing at above 400 °C leads to the formation of globular particles of this phase.

4. The cast billet obtained by the EMC method has a high ductility during cold deformation, which allows drawing a wire with high degrees of deformation (more than 98%).

5. It is shown that 400–450 °C annealing of a cold-rolled strip obtained from a cast billet allows increasing both the electrical conductivity and the hardness. This is due to the formation of Al_3Zr ($L1_2$) phase nanoparticles and, as a result, a decrease of the zirconium concentration in the aluminum solid solution.

Acknowledgements

The study was carried out within the framework of the implementation of the Resolution of the Government of the Russian Federation of April 9, 2010 No. 220 (Contract No. 074-02-2018-329 from May 16, 2018).

REFERENCES

1. ASTM B941-16, Standard specification for Heat Resistant Aluminum-Zirconium Alloy Wire for Electrical Purposes, ASTM International, West Conshohocken, PA, 2016.
2. J.P. Brubak, B. Eftestol, F. Ladiszlaidesz, «Aluminium alloy, a method of making it and an application of the alloy» (IFI CLAIMS Patent Services, 2019), https://patents.google.com/patent/US5067994A/en?oq=5067994. Accessed 30 April 2019.
3. T. Knych, M. Jablonsky, B. Smyrak, *Arch. Metall. Mater*, 54, 671 (2009).
4. I. Properzi, «Machine for the continuous casting of metal rods», (IFI CLAIMS Patent Services, 2019), https://patents.google.com/patent/US2659949A/en?oq=2659949. Accessed 30 April 2019.
5. Information on https://www.southwire.com. Accessed 30 April 2019.
6. N.A. Belov, A.N. Alabin, I.A. Matveeva, D.G. Eskin, *Trans. Nonferrous Met. Soc. China* (2015) doi: 10.1016/S1003-6326(15)63907-3.
7. E. Çadırlı, H. Tecer, M. Sahin, E. Yimaz, T. Kirindi, M. Gündüz, *J. Alloys Compd.* (2015) doi: 10.1016/j.jallcom.2015.01.193.
8. J.D. Robson, P.B. Prangnell, *Acta Mater.* (2001) doi: 10.1016/S1359-6454(00)00351-7.

9. K.E. Knipling, R.A. Karnesky, C.P. Lee, D.C. Dunand, D.N. Seidman, *Acta Mater*. (2010) doi: 10.1016/j.actamat.2010.05.054.
10. A. Deschamp, P. Guyo, *Acta Mater*. (2007) doi: 10.1016/j.actamat.2006.12.015.
11. W. Lefebvre, F. Danoix, H. Hallem, B. Forbord, A. Bostel, K. Marthinsen, *J. Alloys Compd.* (2009) doi: 10.1016/j.jallcom.2008.02.043.
12. B. Forbord, W. Lefebvre, F. Danoix, H. Hallem , K. Marthinsen, *Scripta Mater.* (2004) doi: 10.1016/j.scriptamat.2004.03.033.
13. E. Clouet, A. Barbu, L. Lae, G. Martin, *Acta Mater*, 53, 2313 (2005).
14. N.A. Belov, A.N. Alabin, D.G. Eskin, and V.V. Istomin-Kastrovskiy, *J. Mater. Sci.* (2006) doi: 10.1007/s10853-006-0265-7.
15. N.A. Belov, A.N. Alabin, A.A. Yakovlev, *Izv. Vuzov. Tsvet. Metall. (Proc. Higher Schools Nonferr. Metal)*. (2013) doi: 10.17073/0021-3438-2013-2-50-55.
16. J.W. Evans, *JOM*, 47, Is. 5, 38 (1995).
17. A.A. Avdulov, G.P. Usynina, N.V. Sergeev, I.S. Gudkov, *Tsvet. Met*. (2017) doi: 10.17580/tsm.2017.07.12.
18. V.I. Dobatkin, V.I. Elagin, V.M. Fedorov. *Bystrozakristallizovannye alyuminievye splavy (Rapidly Solidified Aluminum Alloys)*, (Moscow, M: VILS, 1995), pp. 43-59.
19. S.I. Berman. *Proizvodstvo granul iz splavov na osnove alyuminiya i pressovanie iz nih polufabrikatov (Production of granules from aluminum-based alloys and pressing of semi-finished products)*, (Moscow, M: Cvetmetinformaciya, 1971), pp. 101
20. I.J. Polmear, *Light Metals: From Traditional Alloys to Nanocrystals*, 4th ed. (Oxford, UK: Elsevier, 2006), pp. 188-193.
21. G. Zeer, M.V. Pervukhin, E.G. Zelenkova, *Met. Sci. Heat Treat.* (2011) doi: 10.1007/s11041-011-9370-6.
22. N.A. Belov, D.G. Eskin, A.A. Aksenov, *Multicomponent phase diagrams: applications for commercial aluminum alloys*, (Amsterdam, NL: Elsevier, 2005), pp. 19-31.
23. M.V. Glazoff, A.V. Khvan, V.S. Zolotorevsky, N.A. Belov, Alan T. Dinsdale, *Casting Aluminum Alloys. Their Physical and Mechanical Metallurgy.* (Oxford, UK: Elsevier, 2019), pp. 180-186.
24. J.E. Hatch, ed., *Aluminum—Properties and Physical Metallurgy* (Metals Park, OH: ASM, 1984), pp. 59-64.
25. C. Booth-Morrison, Z. Mao, M. Diaz, D.C. Dunand, C. Wolwerton, D.N. Seidman, *Acta Mater*. (2012) doi: 10.1016/j.actamat.2012.05.036.
26. N.A. Belov, N.O. Korotkova, A.N. Alabin, S. S. Mishurov, *Russ. J. Non-ferrous Metals.* (2018) doi: 10.3103/S1067821218030033.

27. T. Gao, A. Ceguerra, A. Breen, X. Liu, Yu. Wu, S. Ringer, *J. Alloys Comd*. (2016) doi: 10.1016/j.jallcom.2016.02.236.
28. Information on http://www.npcmgd.com. Accessed 25 April 2019
29. Information on www.thermocalc.com. Accessed 30 March 2019
30. N.A. Belov, A.N. Alabin, A.Yu. Prokhorov, *Russ. J. Non-ferrous Metals.* (2009) doi: 10.3103/S1067821209040099.
31. L. Bäckerud, G. Chai, J. Tamminen. *Solidification Characteristics of Aluminum Alloys. Vol. 1: Foundry Alloys*, (Oslo, NO: Skanaluminium, 1986), pp. 9-26.
32. N.A. Belov, A.A. Aksenov, D.G. Eskin, *Iron in aluminum alloys: impurity and alloying element*, (London, UK: Fransis and Tailor, 2002). 360 p.
33. A. Školáková, P. Novák, D. Vojtěch, T.F. Kubatík, *Mater. Des.* (2016) doi: 10.1016/j.matdes.2016.06.069.
34. H. Chen, Q. Chen, Y. Du, J. Brataberg, A. Engstrom, Update of Al−Fe−Si, Al−Mn−Si and Al−Fe−Mn−Si thermodynamic descriptions [J]. Trans. Nonferrous Met. Soc. China (2014) doi: 10.1016/S1003-6326(14)63310-0.
35. Y.Nasedkina, X. Sauvage, E.V. Bobruk, M. Yu. Murashkin, R.Z. Valiev, N.A. Enikeev, *J. Alloys Comd*. (2017) doi: 10.1016/j.jallcom.2017.03.312 0925-8388

Fig1a

Click here to access/download;Figure;FIG-1a.jpg

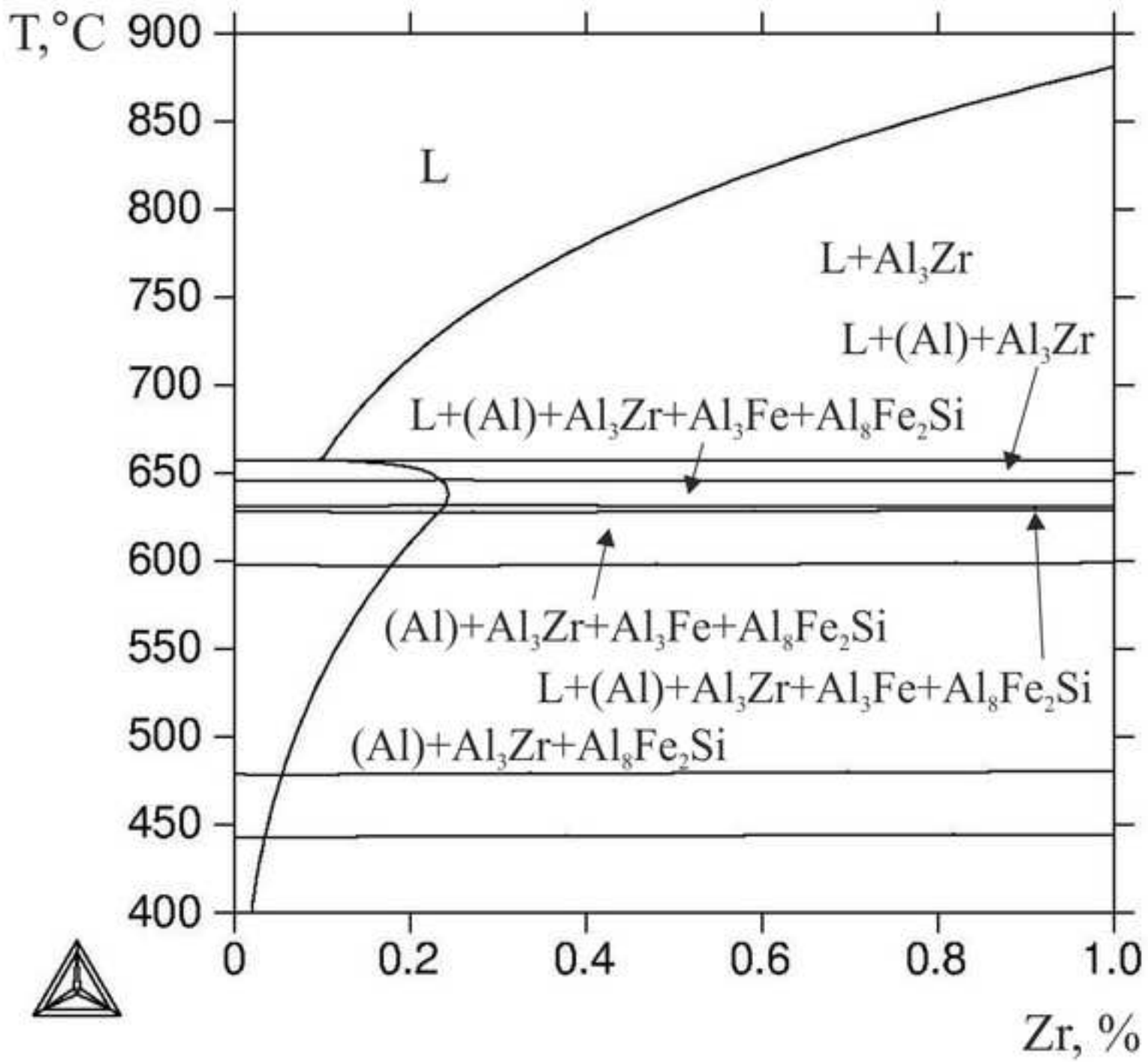

Fig1b

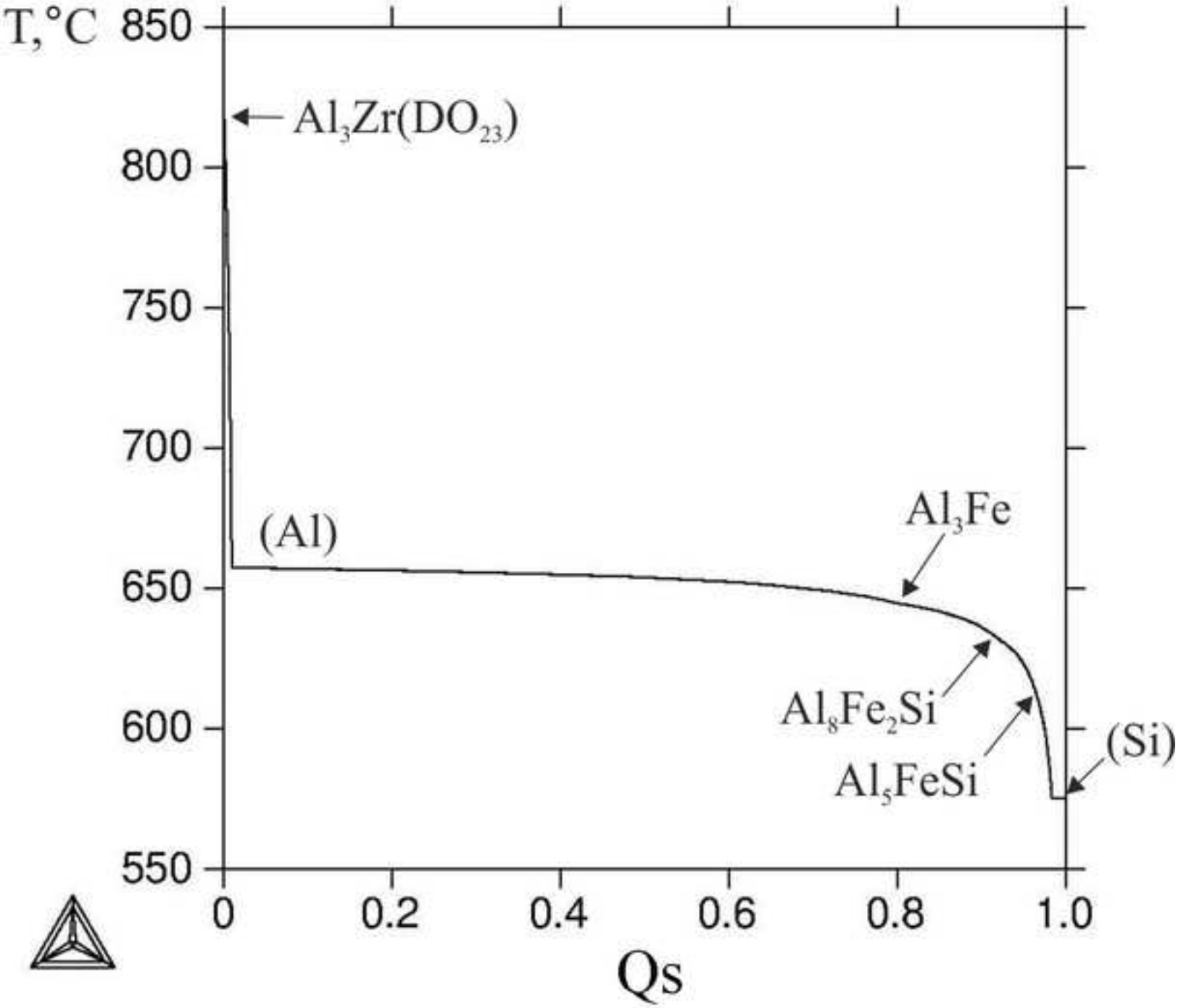

Fig1c

Click here to access/download;Figure;FIG-1c.jpg

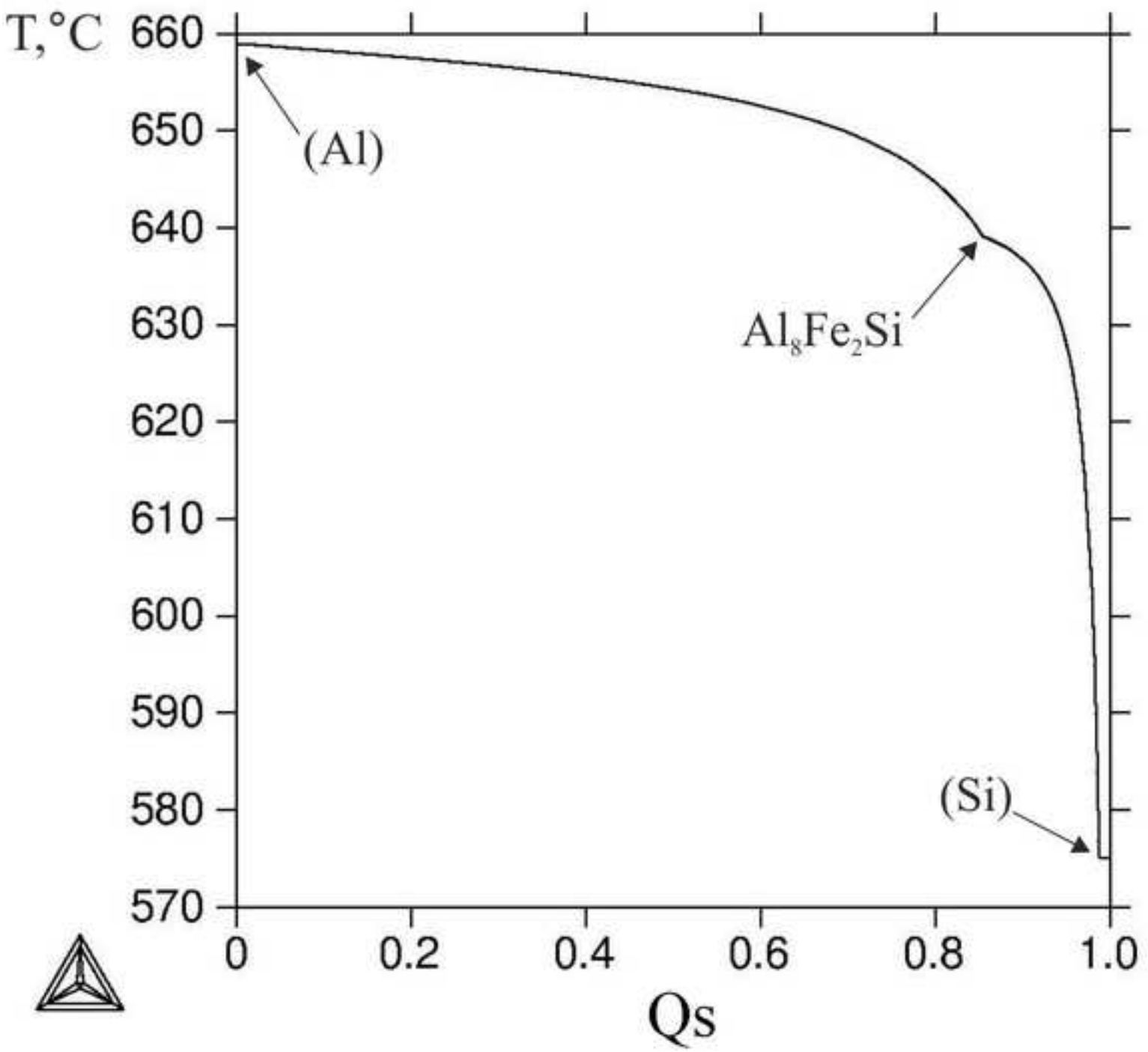

Fig2a

Click here to access/download;Figure;FIG-2a.tif

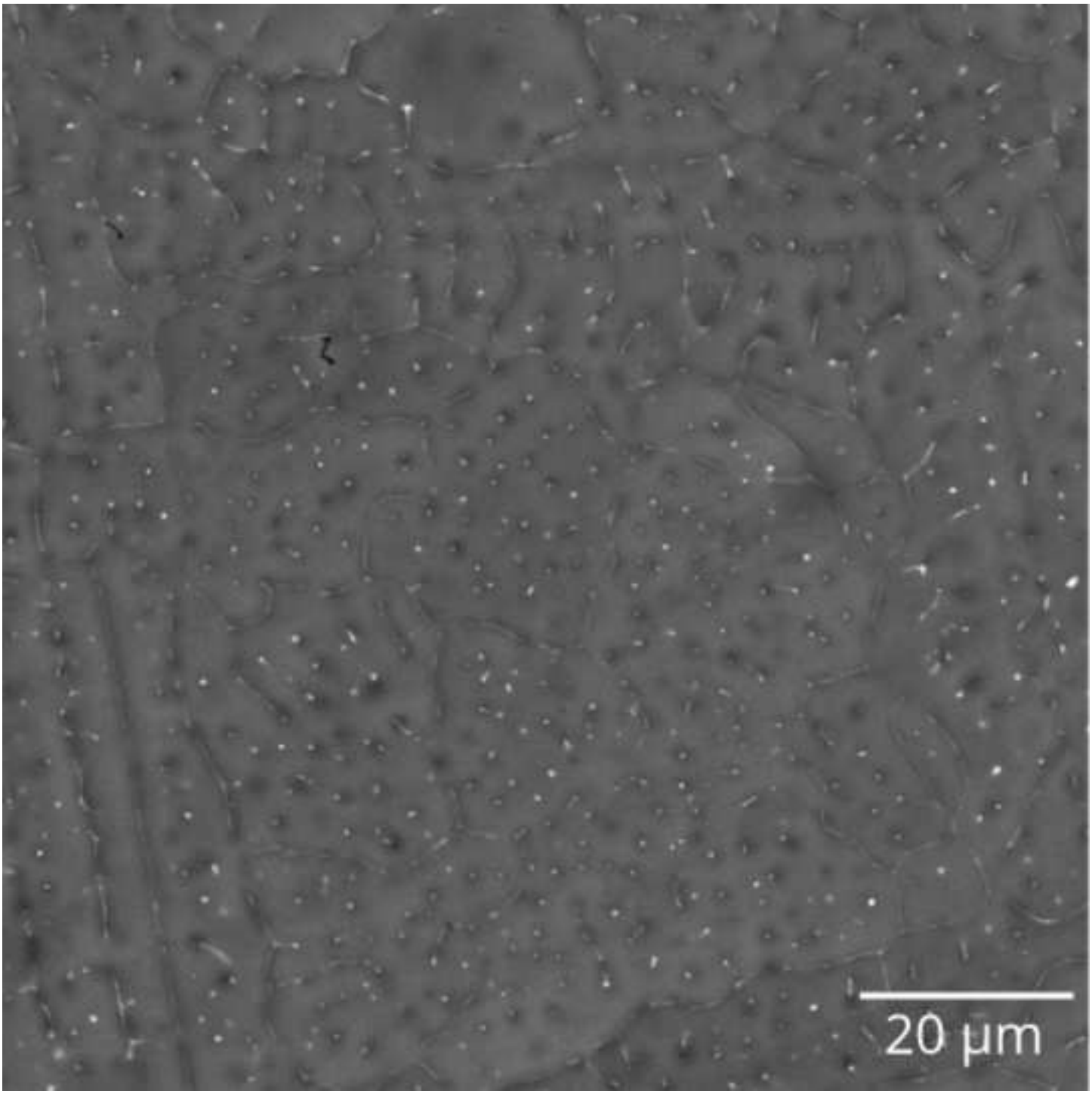

Fig2b

Click here to access/download;Figure;FIG-2b.tif

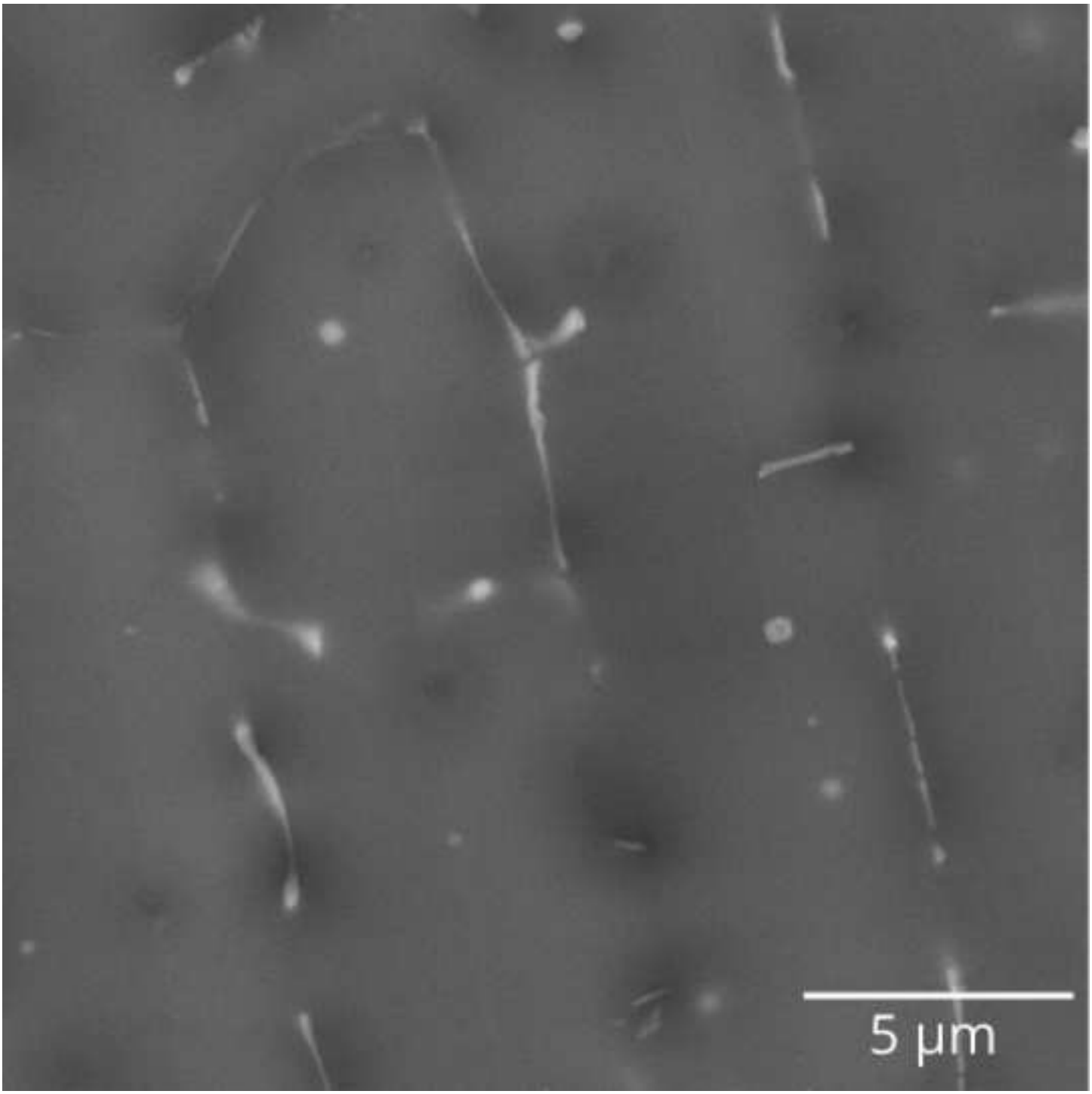

Fig2c

Click here to access/download;Figure;FIG-2c.tif

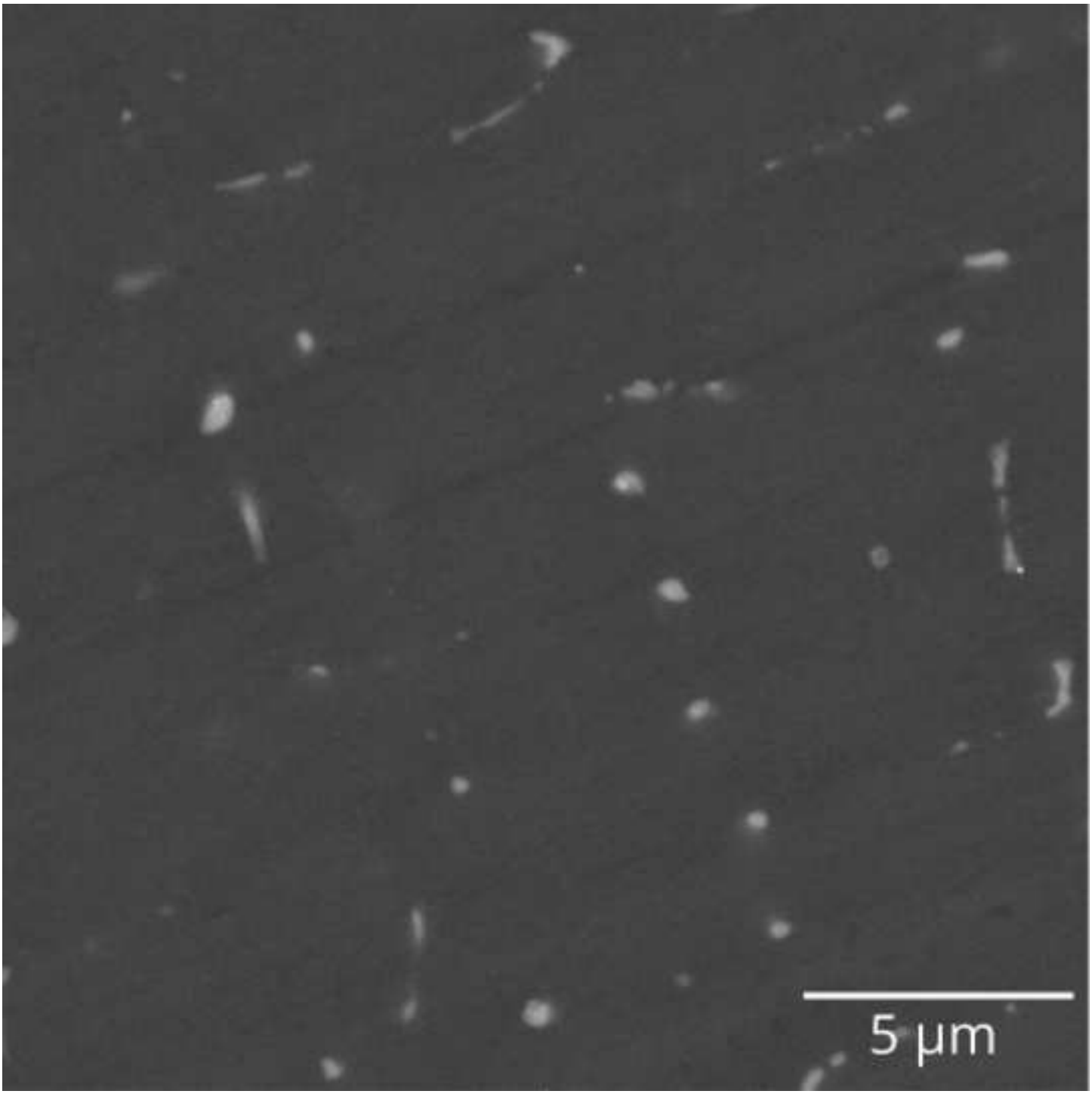

Fig2d

Click here to access/download;Figure;FIG-2d.tif

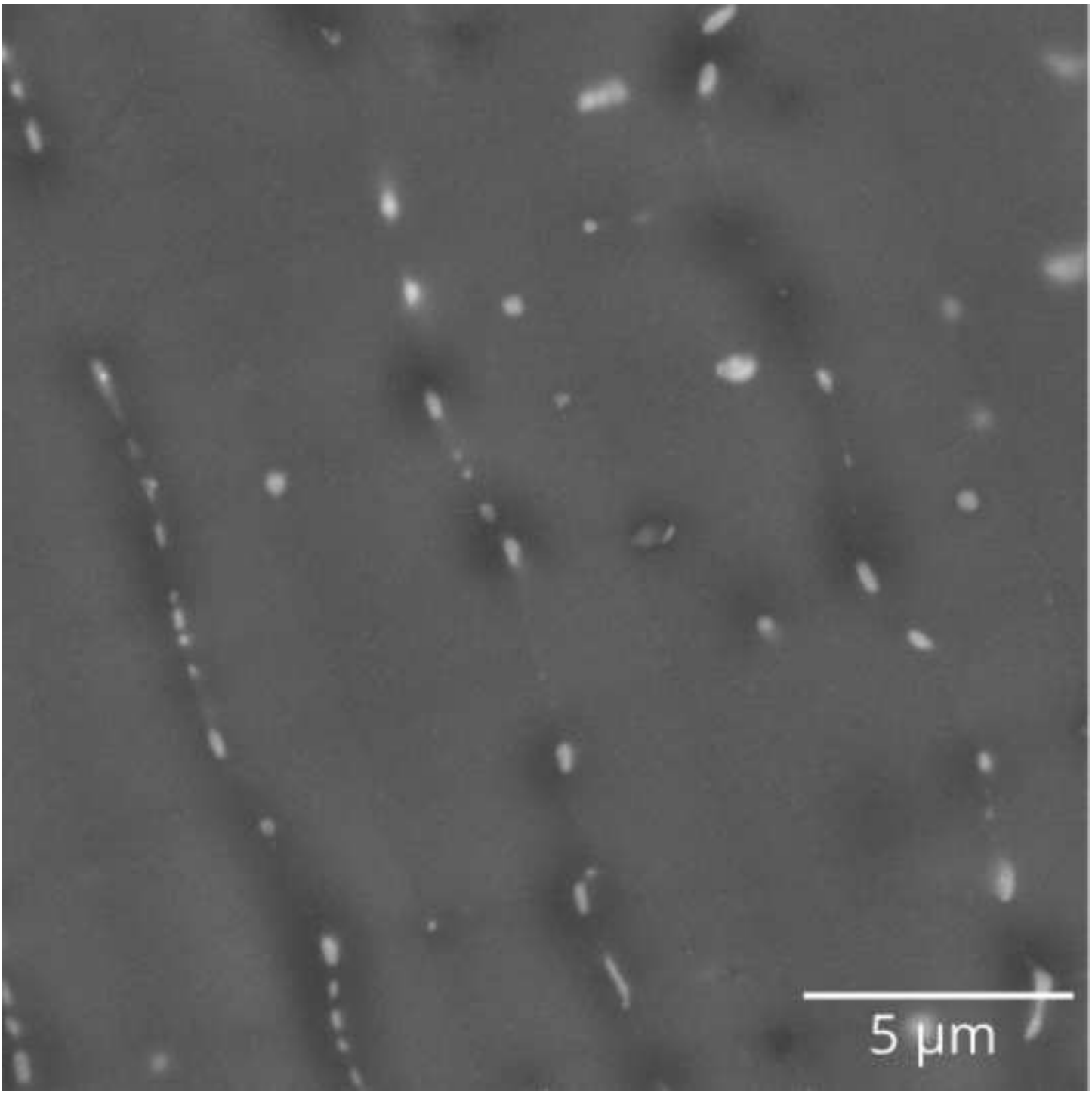

Fig2e

Click here to access/download;Figure;FIG-2e.tif

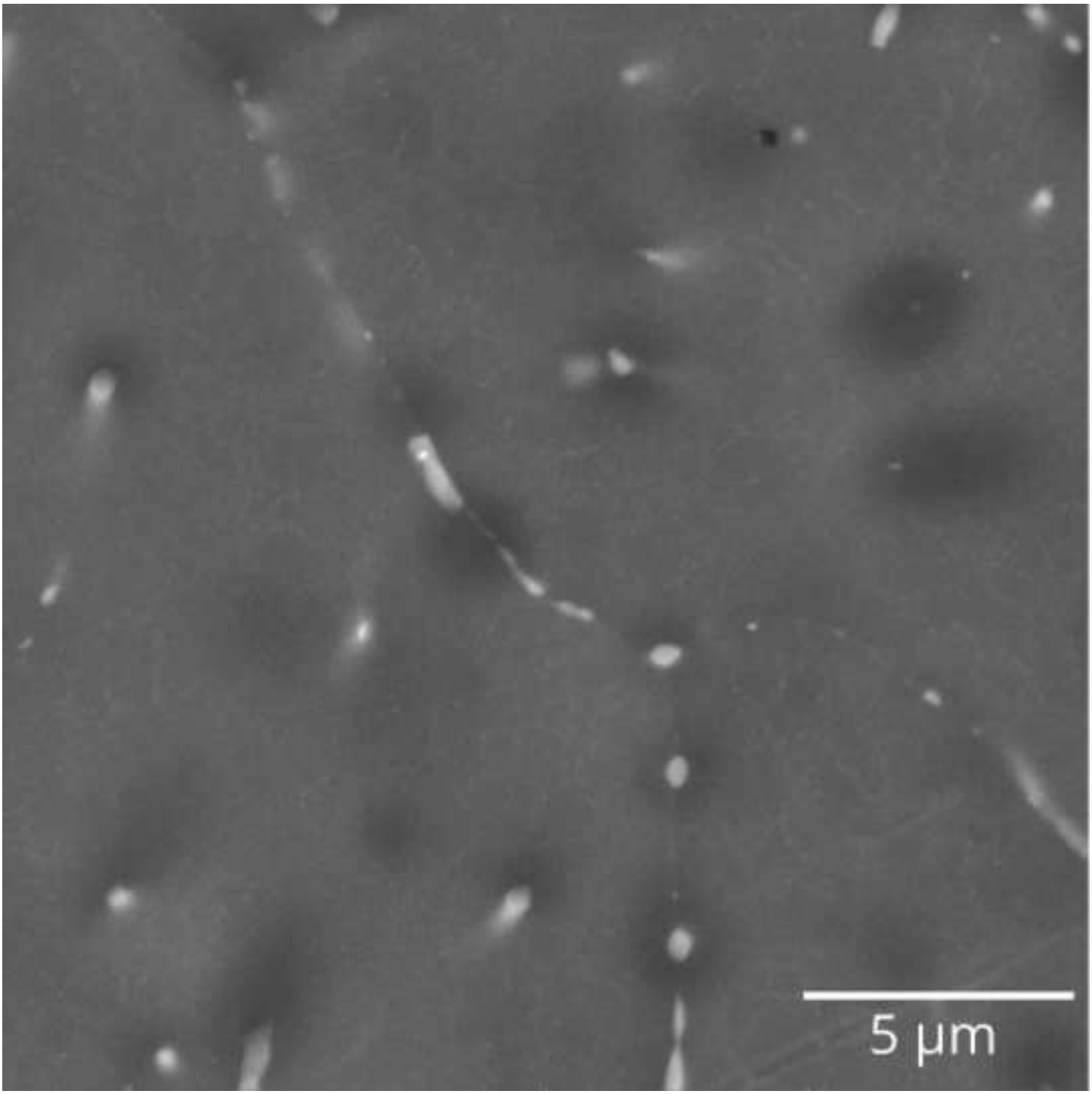

Fig2f

Click here to access/download;Figure;FIG-2f.tif

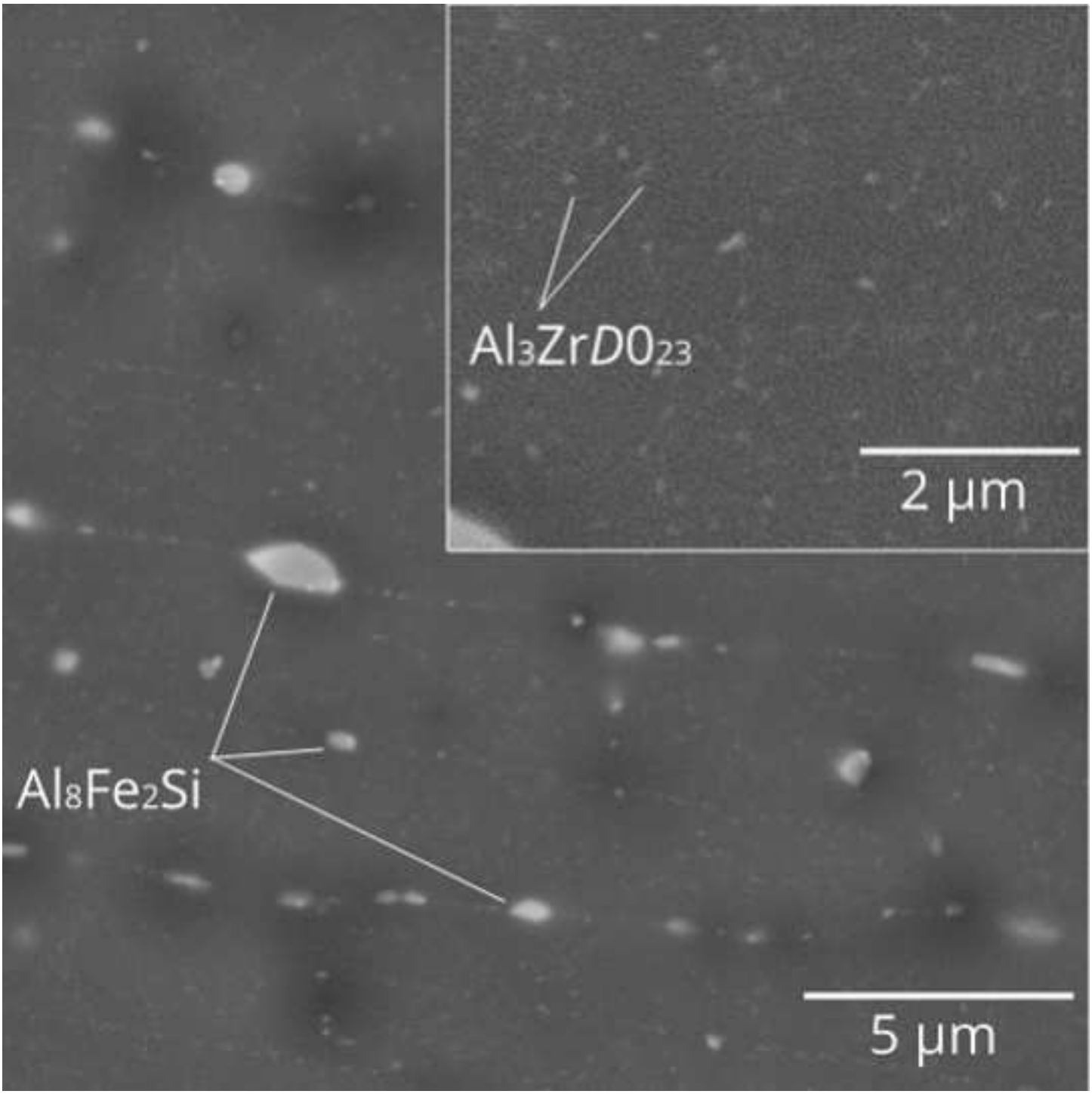

Fig3a

Click here to access/download;Figure;FIG-3a.tif

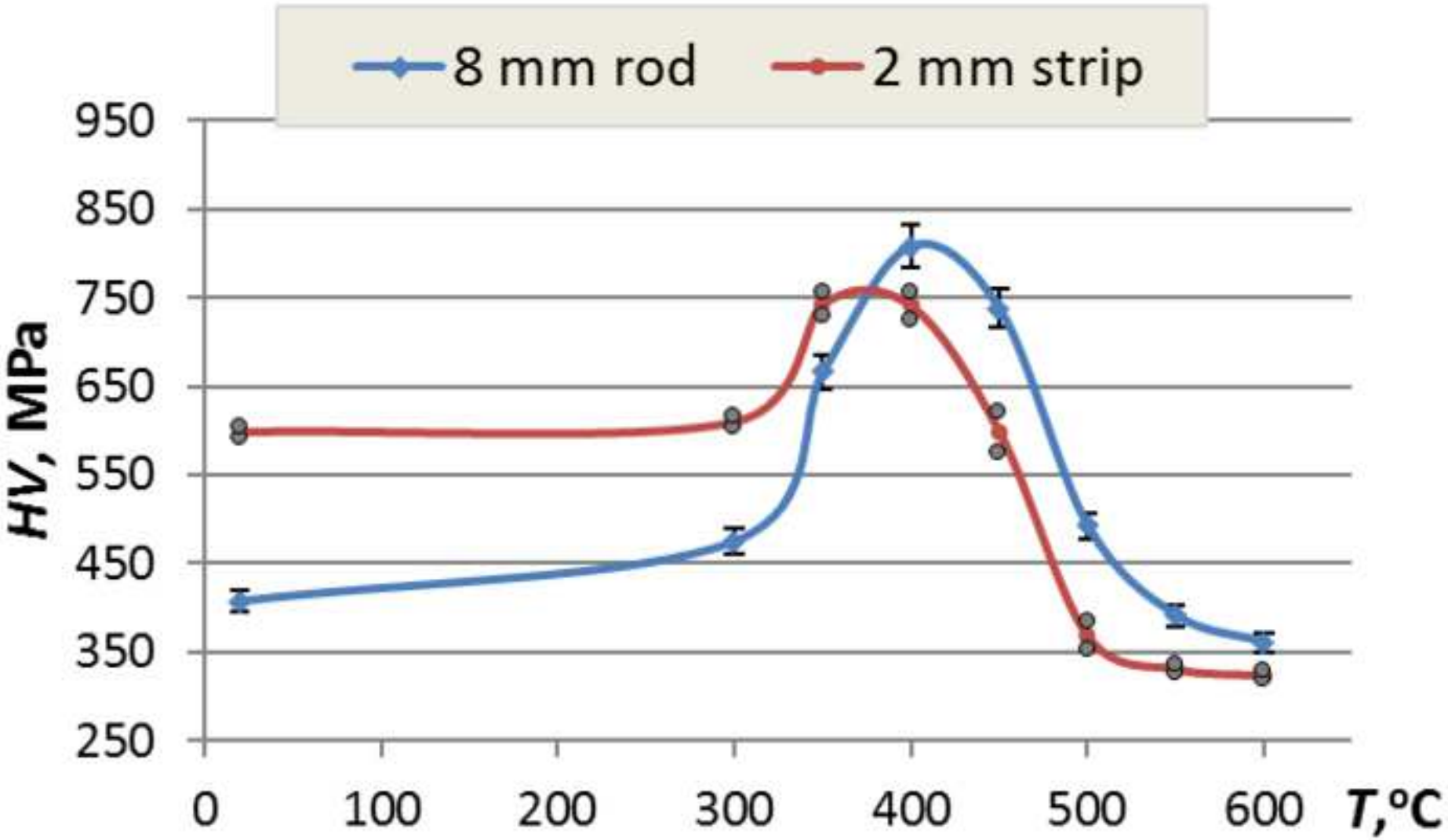

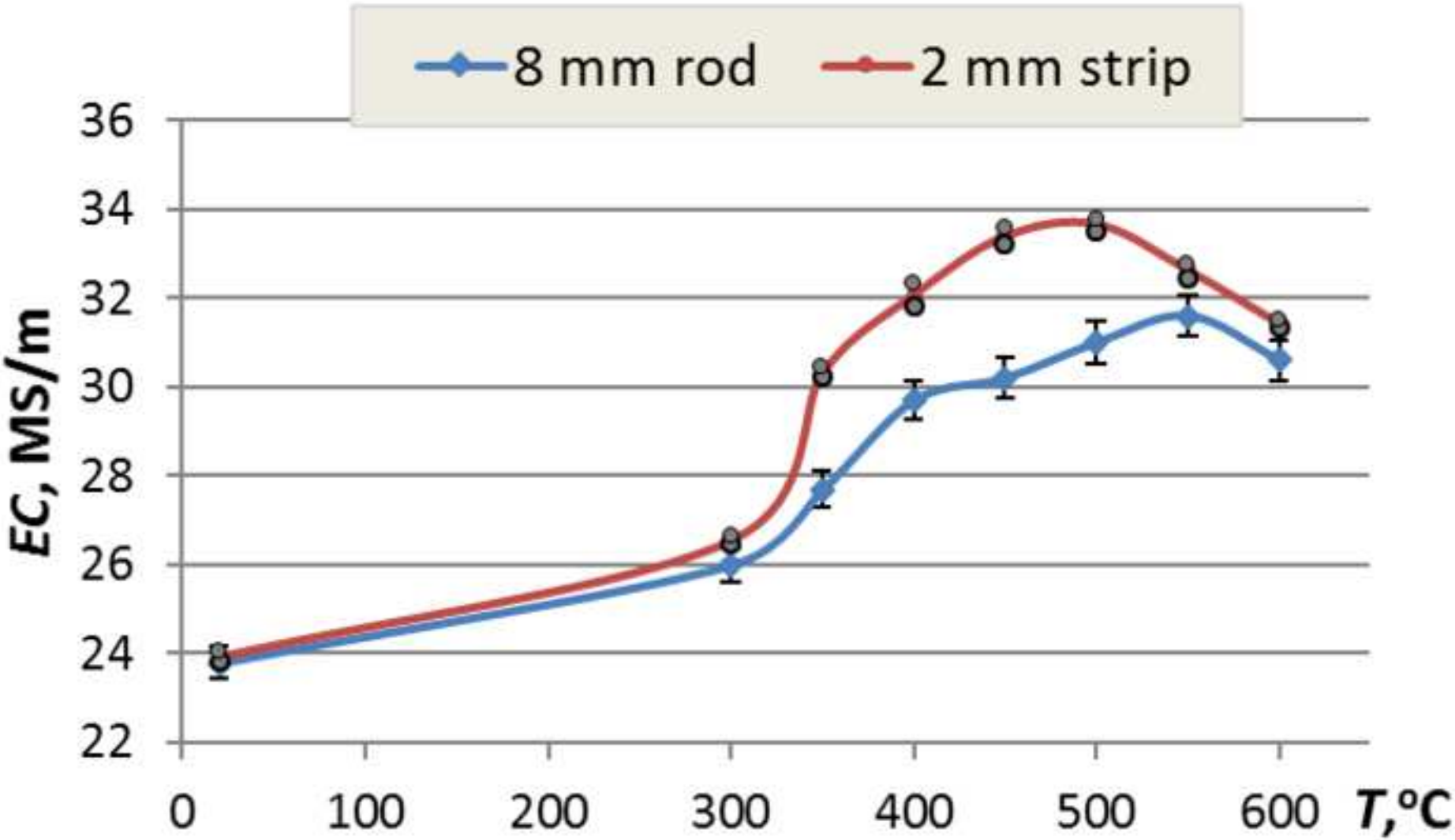

Fig4a

Click here to access/download;Figure;FIG-4a.jpg

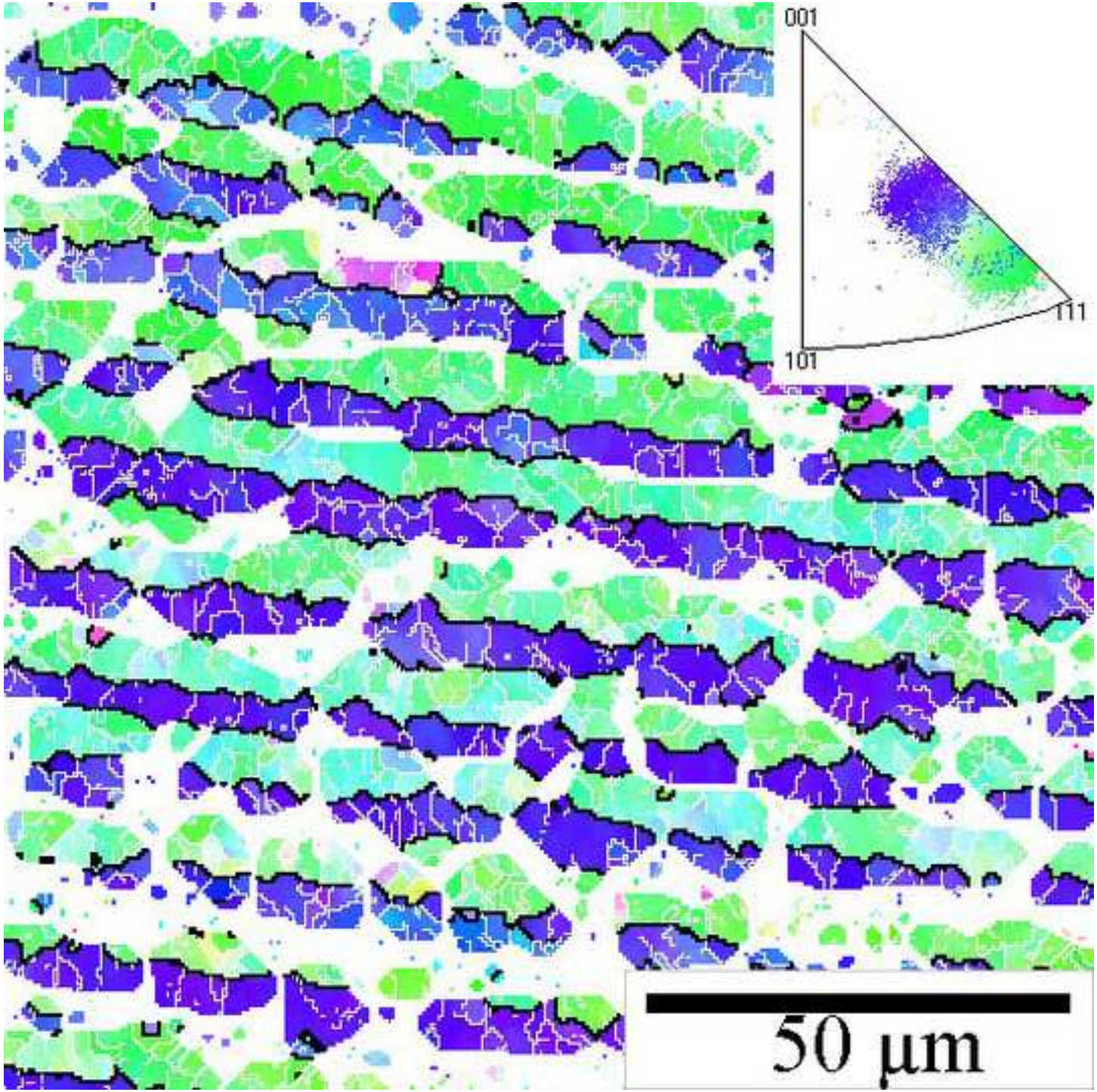

Fig4b

Click here to access/download;Figure;FIG-4b.jpeg

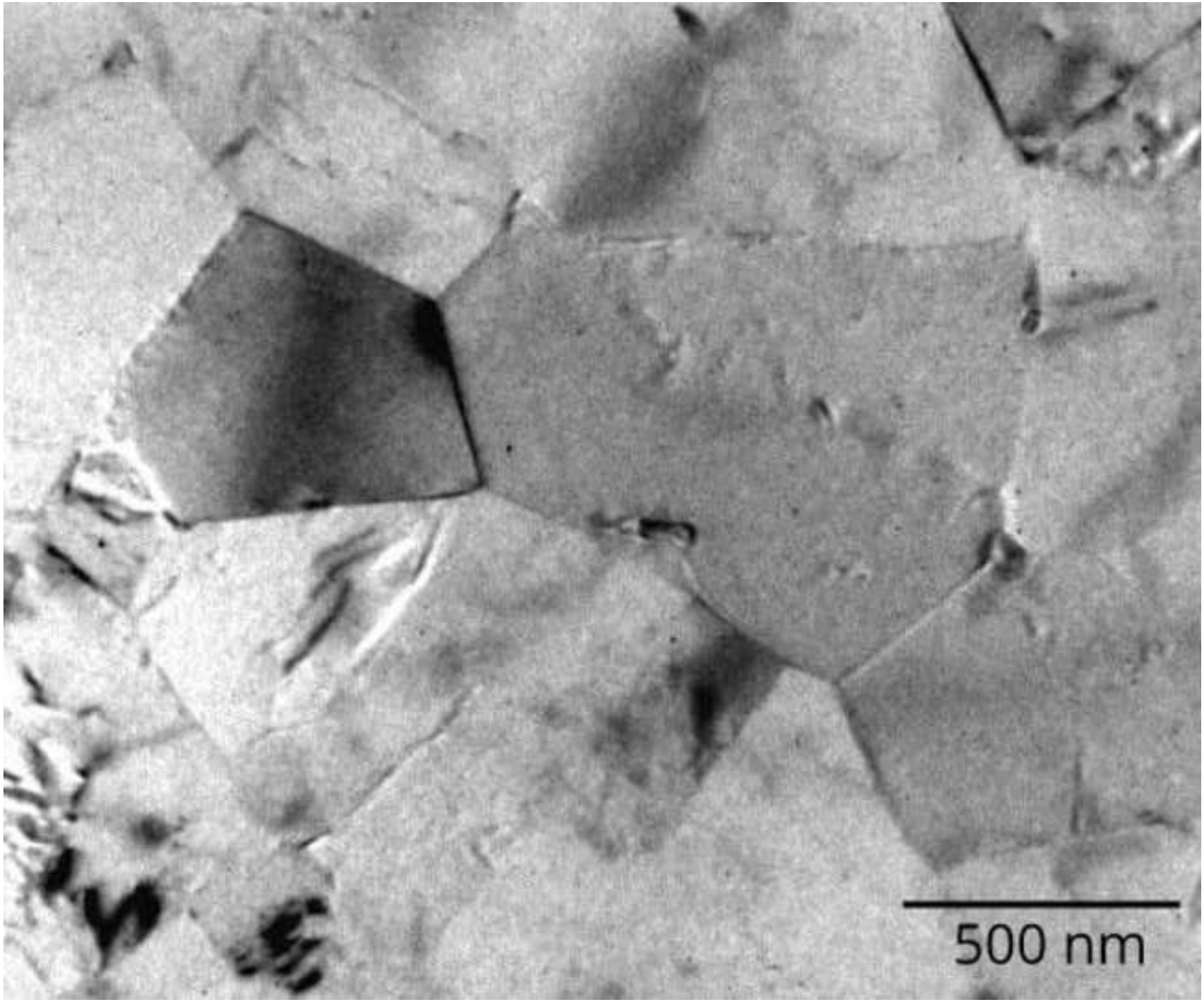

Fig4c

Click here to access/download;Figure;FIG-4c.jpeg

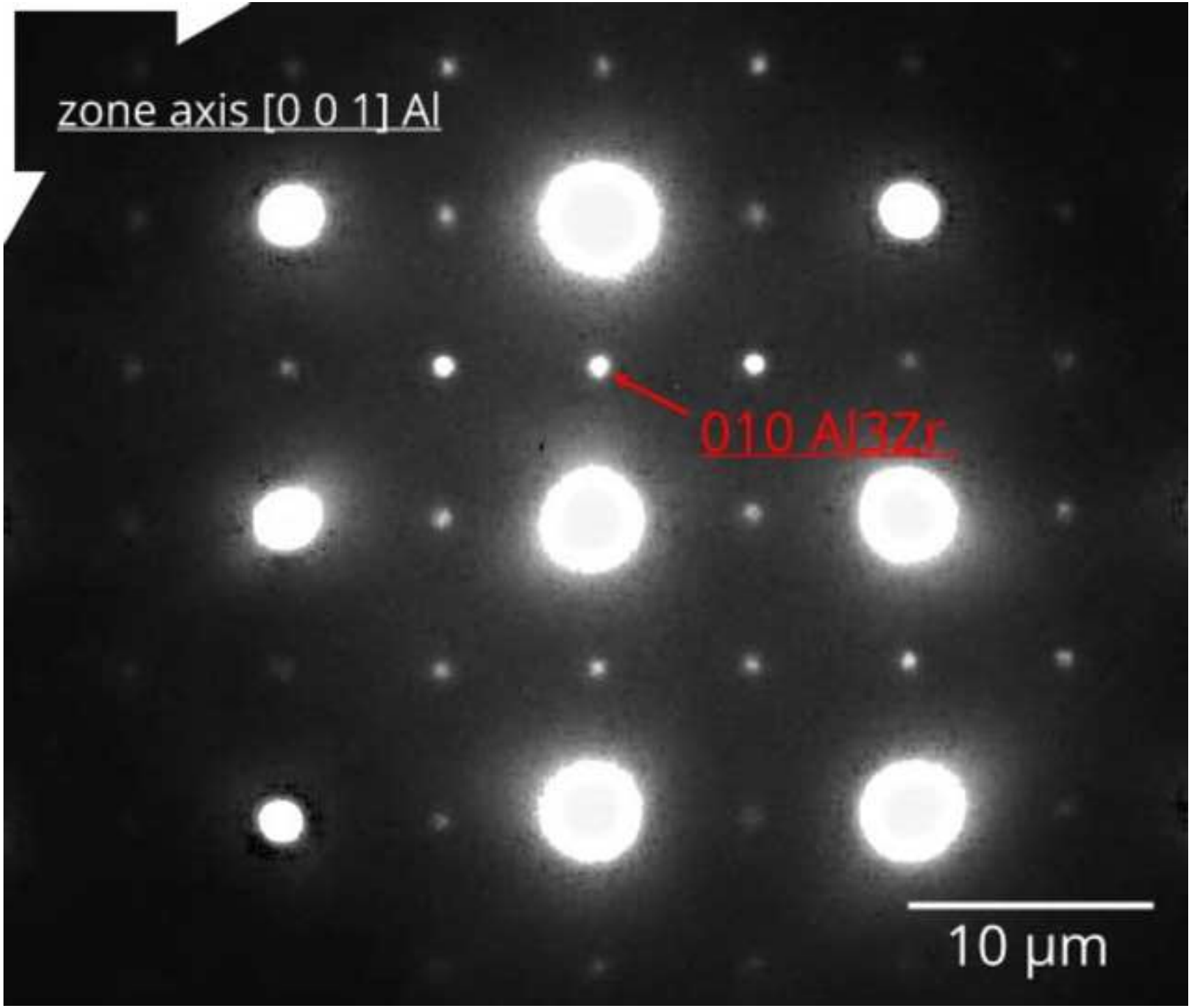

Fig4d

Click here to access/download;Figure;FIG-4d.jpg

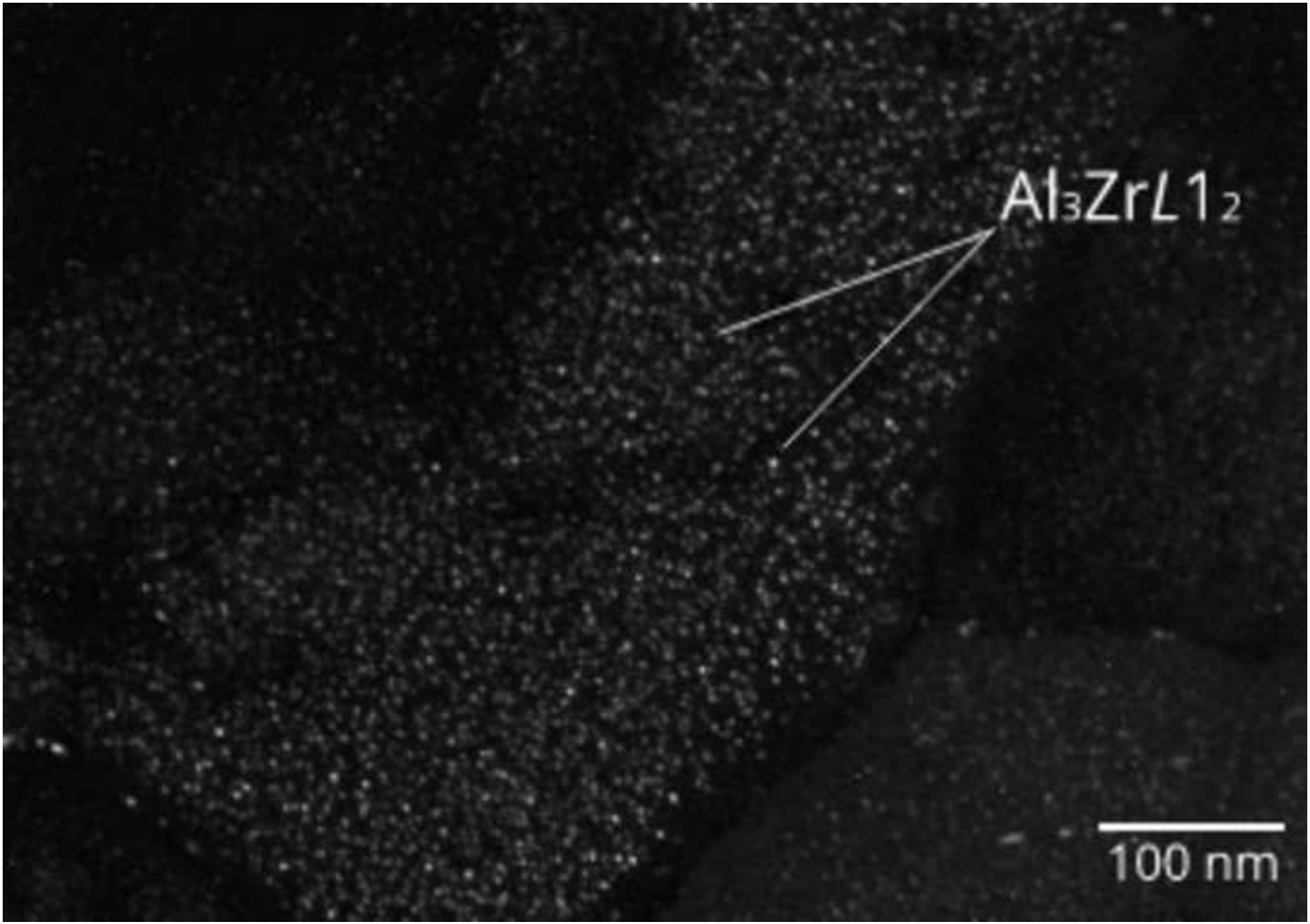

Fig5a

Click here to access/download;Figure;FIG-5a.tif

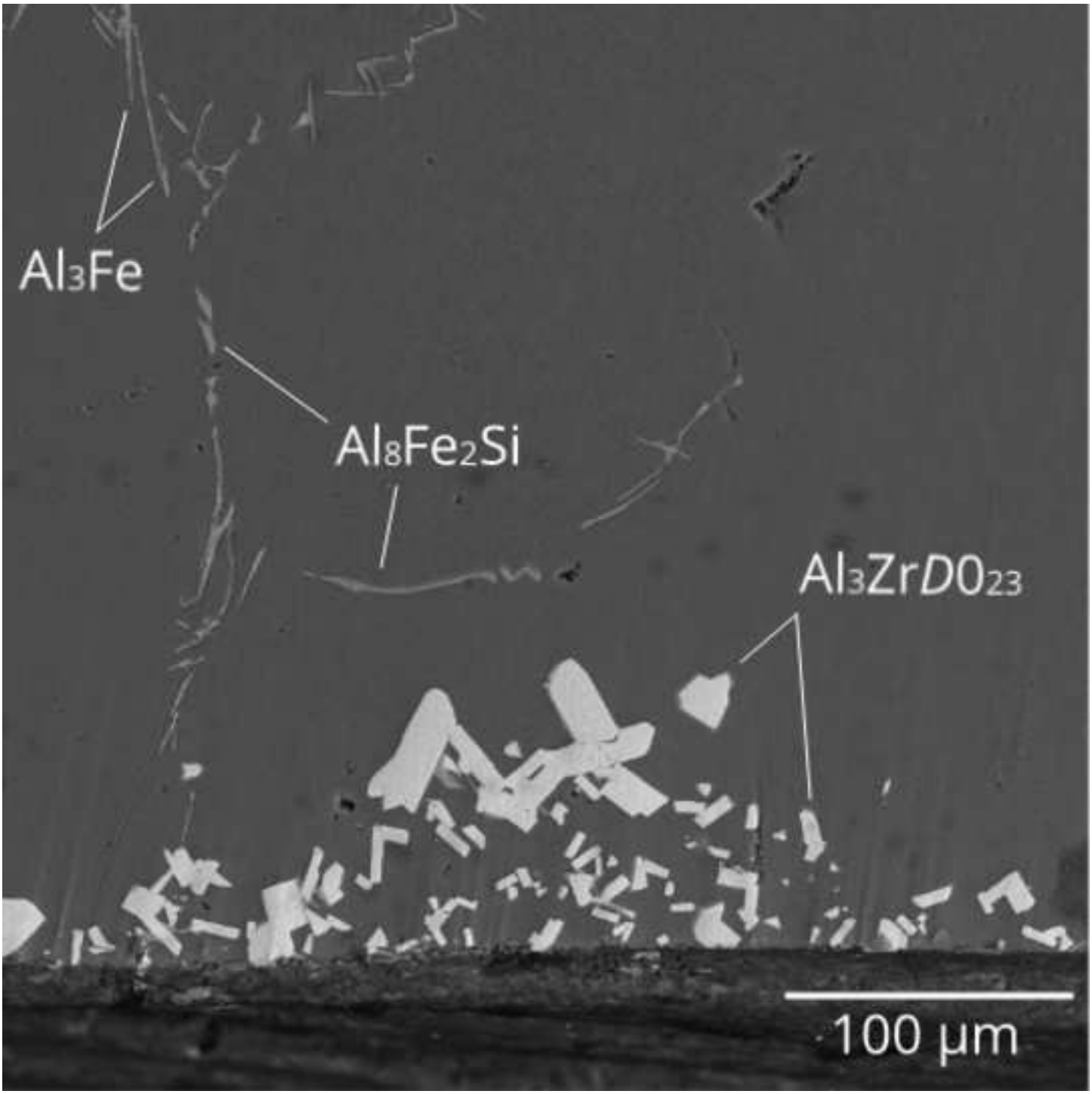

Fig5b

Click here to access/download;Figure;FIG-5b.tif

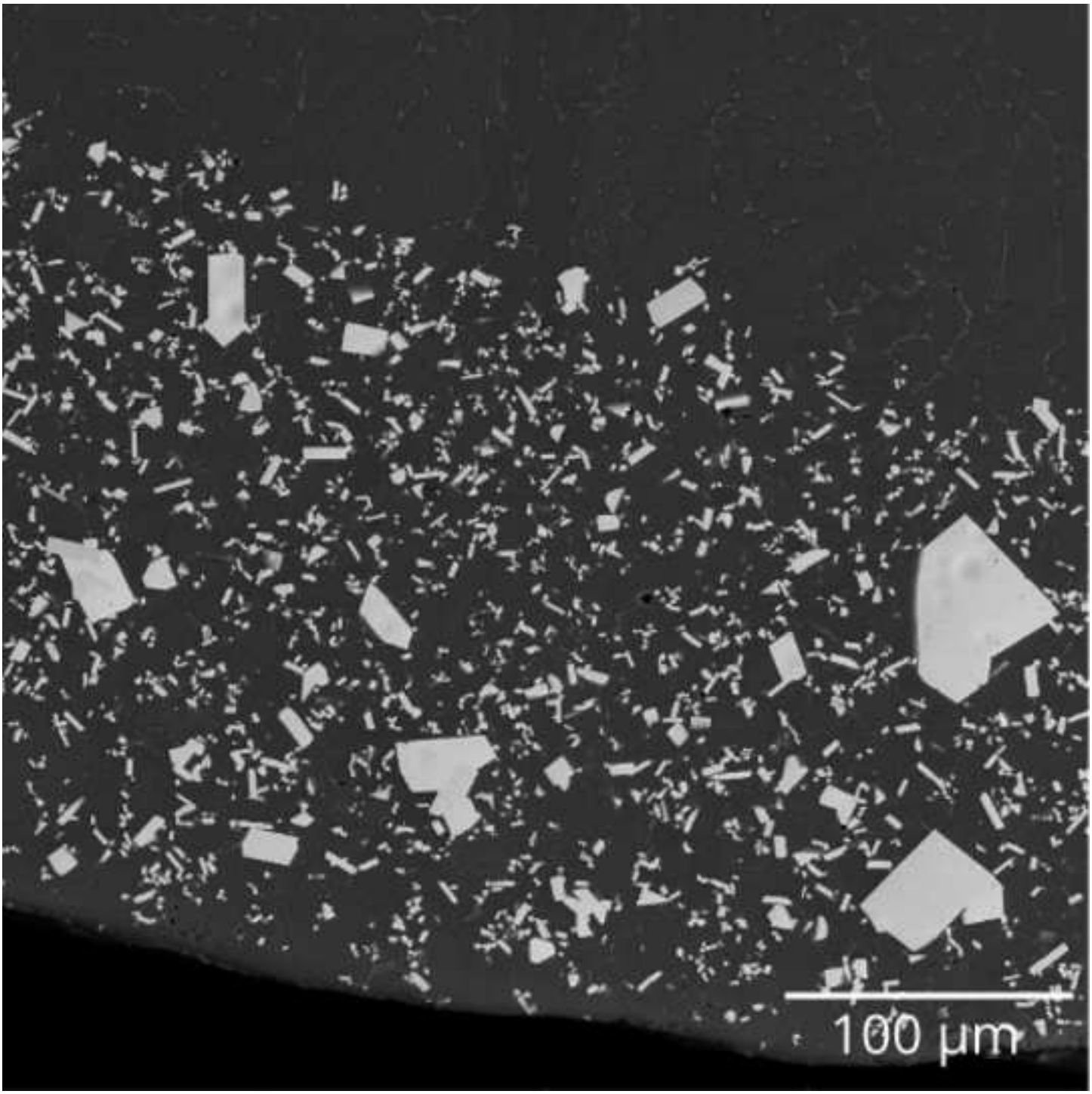

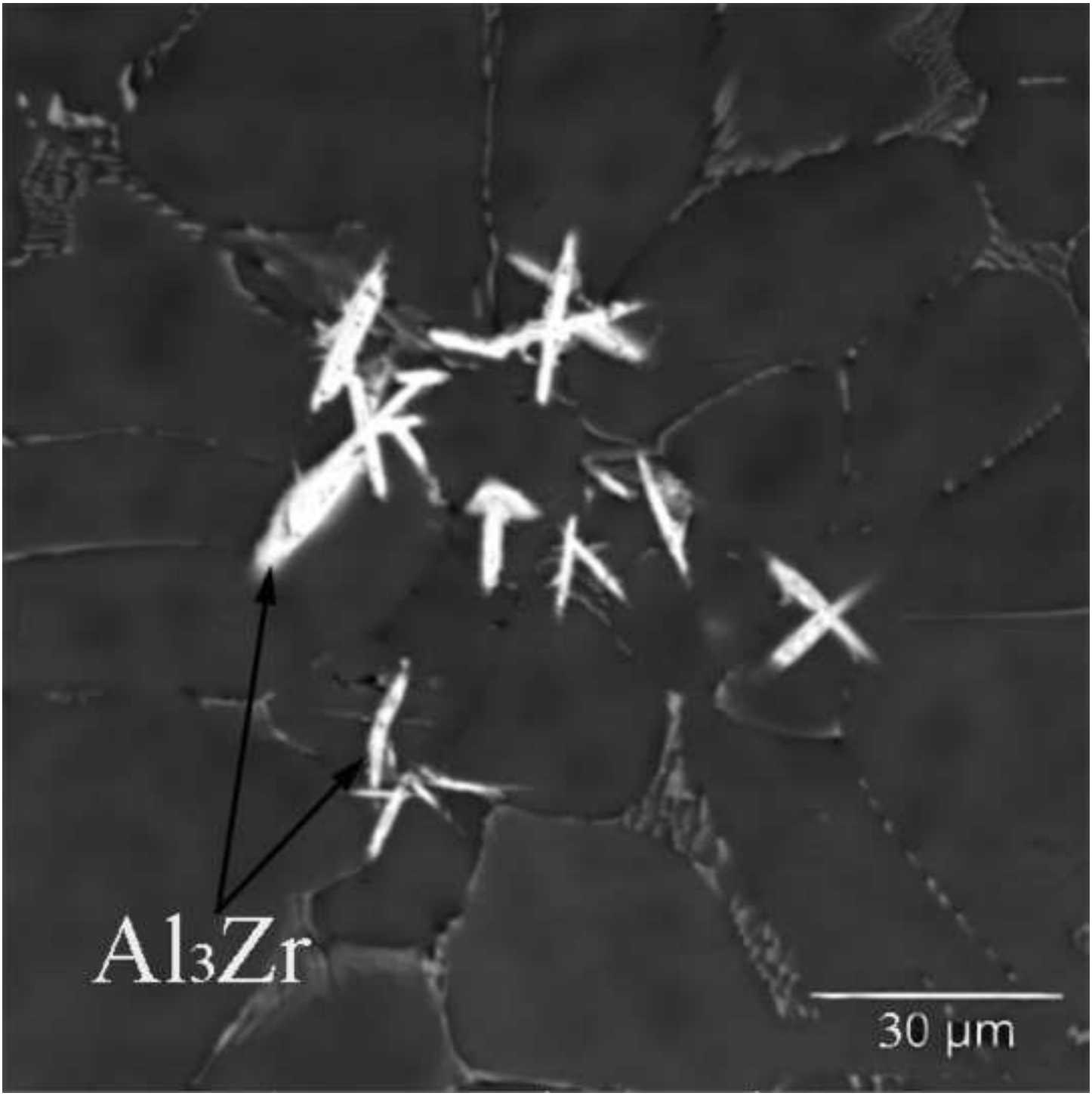

Structure and Properties of Al–0.6%Zr–0.4%Fe–0.4%Si (wt%) Wire Alloy Manufactured by Electromagnetic Casting

Nikolay A. Belov[1], Natalia O. Korotkova[1], Torgom K. Akopyan[1,2], Viktor N.Timofeev[3]

[1]National University of Science and Technology MISiS, 4 Leninsky pr., Moscow, 119049, Russia

[2]Baikov Institute of Metallurgy and Materials Science, 49 Leninsky pr., Moscow, 119991, Russia

[3]Siberian Federal University, 79 Svobodnyy prospekt., Krasnoyarsk, 660041, Russia

Abstract

The experimental Al–0.6%Zr–0.4%Fe–0.4%Si alloy has been manufactured by using the method of electromagnetic casting (EMC). It is shown that Zr is completely dissolved in the aluminum solid solution (Al) and iron is fully included in the Al_8Fe_2Si phase. The fine microstructure of the as-cast rod implies a high deformation plasticity, which has been experimentally confirmed during wire production. The cold rolled wire has UTS ~ 260 MPa and subsequent annealing at 400 °C for 3 h. slightly reduces the strength which is associated with the stabilizing effect of the $L1_2$ (Al_3Zr) phase nanoparticles formed during annealing. Annealing also leads to a significant increase in the specific conductivity, the value of which reaches 57.0 IACS. Drawing of the annealed rolled wire leads to significant strengthening. Annealing at 400 ^{0}C leads to a marked strength reduction, which, however, remains high enough for conductive alloys (UTS higher than 200 MPa).

Keywords: Aluminum-zirconium alloys; electrical conductivity, electromagnetic casting, phase composition, mechanical properties

Corresponding author: Torgom Akopyan **Email:** nemiroffandtor@yandex.ru

1. Introduction

Aluminum alloys of the Al–Zr system are widely used in thermally stable cable products that should combine high electrical conductivity and sufficient strength preserved after heating to ~300 °C [1-3]. Wire rods for electrical cables are typically manufactured by using of a complex of continuous casting and rolling (CCR). The most popular companies providing such equipment are well known “Continuus-Properzi” [4] and “Southwire” [5]. The desired characteristics of Al-Zr wire (first of all, electrical conductivity, strength and thermal stability) depend considerably on the processing parameters of wire rods, which includes zirconium concentration, casting conditions, rolling regime and, most importantly, the heat treatment cycle [6]. According to the experimental results for the conductivity of alloys containing 0.2–0.3% Zr (hereinafter wt.% unless otherwise stated) the peak values occur after annealing at 350–400 °C for hundreds of hours [7, 8]. Optimization of the CCR process is a difficult task due to its complexity compared to conventional processing which is characterized by time and space separated processes used for ingot production and subsequent deformation.

Positive influence of zirconium on the thermal stability is caused by nanoparticles of the $L1_2$ (Al_3Zr) phase formed in wire rods as a result of the decomposition of a supersaturated aluminum solid solution (hereinafter (Al)) during annealing [9-15]. As shown earlier [9], these nanoparticles start to precipitate at between 350 and 375 °C, achieving peak hardening at 400–450 °C. It was shown [6] that an increase in the zirconium content from 0.2 to 0.5 % leads to a significant increase in the thermal stability without a decrease in the electrical conductivity. Since zirconium sharply increases the liquidus temperature, the melting and casting temperatures of those alloys should be significantly higher compared to conventional ones, which is not always achievable in industrial production, including the CCR technology.

In our opinion, a promising technology for the production of conductive aluminum alloys with a high concentration of zirconium (more than 0.5%) is the method of electromagnetic casting (EMC) which allows producing long ingots with small cross section [16,17]. The EMC technology provides casting at a sufficiently high temperature (up to 900 °C) and ultra-high solidification rates (10^3 –10^4 K/s). This allows achieving the same structure as in the alloys produced with the RS / PM technology (rapid solidification / powder metallurgy) [18-20]. The good promise of the EMC method has been demonstrated for the production of conductive aluminum alloys containing about 7% RE [21] which were previously developed specifically for RS / PM technology [18].

Some strengthening of aluminum alloys without a significant reduction in their electrical conductivity can be achieved by adding iron in an amount of up to 1%, which is implemented in

a number of branded alloys (for example, 8076). In terms of the best plasticity, (this is important for providing the necessary manufacturability during drawing), the most favorable morphology among the iron phases has the Al_8Fe_2Si phase, the formation of which requires a certain amount of silicon [22-24]. The presence of iron and silicon in alloy is also advisable from the viewpoint of cost reduction since these elements are the main impurities in commercial aluminum. Silicon is usually an undesirable impurity in the conductive alloys, however, according to some data, this element accelerates the precipitation of the Zr-containing phase during annealing [25-27].

Thus, based on the above, the aim of this work was to substantiate the promise of the EMC method for producing conductor alloys based on the Al – Zr – Fe – Si system containing at least 0.5% Zr.

2. Experimental methods

The chemical composition of the experimental alloy obtained by the EMC (Oxford Instruments) method was the Al–0.62%Zr–0.41%Fe–0.39%Si (throughout the article, the content of elements is indicated in wt.% (unless otherwise specified)). The equipment of Research and Production Centre of Magnetic Hydrodynamics was used [28]. The melting was carried out in an induction furnace in a graphite-chased crucible based on commercial aluminum (99.5 wt.%). Zr, Fe and Si were introduced into the aluminum melt in the form of master alloys (Al-5%Zr, 80%Fe-20%flux and Al–12%Si) at ~850 °C. The casting was carried out by the EMC method at a temperature of ~830 °C in order to obtain the long-length cast rod with a diameter of 8 mm and a length of ~20 m. For laboratory rolling, a 0.5 m long sample was cut from the EMC rod.

By using laboratory rolls of VEM-3SM, wire with a square cross-section of 1x1 mm was obtained at room temperature from the as-cast EMC rod (the reduction ratio was 98 %). Thus, the rolling of the rod was carried out without preliminary annealing or heating of the ingot. From this wire, after intermediate annealing at 400 ^{0}C, wires with diameters of 0.5 mm and 0.26 mm were obtained by drawing (the reduction degrees were 80% and 95% respectively). The resulting wire was studied in the as-drawn state and after annealing at 400°C. The main stages of the processing route are summarized in Table 1. Additionally a 2 mm strip was obtained by cold rolling of the as-cast EMC billet for studying the effect of the annealing temperature on the hardness and electrical conductivity (EC). The diagram of the thermomechanical routings is presented in supplementary materials (refer to online supplementary material, Fig. S-1).

The microstructure was examined by means of scanning electron microscopy (SEM, TESCAN VEGA 3), electron microprobe analysis (EMPA, OXFORD AZtec) and transmission electron microscopy (TEM, JEM−2100). Polished samples were used for the studies. Mechanical

polishing was used, as well as electrolytic polishing, which was carried out at a voltage of 12 V in an electrolyte containing six parts C_2H_5OH, one part $HClO_4$ and one part glycerine. The thin foils for TEM were prepared by ion thinning with a PIPS (Precision Ion Polishing System, Gatan) machine and studied at 160 kV. Additionally the microstructure of the experimental alloy was examined after slow solidification (in the furnace) from 850 ^{0}C and after rapid solidification (in water) from 750 ^{0}C.

Table 1 Deforming and heating treatment of the experimental alloy

Designation	Regime
EMC rod (diameter 8 mm)	
R0	As-cast
R300	Annealing at 300 ^{0}C for 3 h
R350	R300 + annealing at 350 ^{0}C (3 h)
R400	R350 + annealing at 400 ^{0}C (3 h)
R450	R400 + annealing at 450 ^{0}C (3 h)
R500	R450 + annealing at 500 ^{0}C (3 h)
R550	R500 + annealing at 550 ^{0}C (3 h)
R600	R550 + annealing at 600 ^{0}C (3 h)
Cold rolled EMC rod to strip (thickness 2 mm)	
S0	Cold rolled strip
S300	Annealing at 300 ^{0}C for 3 h
S350	S300 + annealing at 350 ^{0}C (3 h)
S400	S350 + annealing at 400 ^{0}C (3 h)
S450	S400 + annealing at 450 ^{0}C (3 h)
S500	S450 + annealing at 500 ^{0}C (3 h)
S550	S500 + annealing at 550 ^{0}C (3 h)
S600	S550 + annealing at 600 ^{0}C (3 h)
Wires produced from as-cast EMC rod	
W1	Cold rolling of 8 mm rod to 1 mm wire (reduction 98%)
W1-400	Annealing of 1 mm wire at 400 ^{0}C during 3 hours
W0.5	Drawing of 1mm wire (annealed at 400 ^{0}C) to 0.5 mm (reduction 80%)
W0.26	Drawing of 1mm wire (annealed at 400 ^{0}C) to 0.26 mm (reduction 95%)
W0.5-400	Annealing of 0.5 mm wire at 400 ^{0}C during 1 hours
W0.26-400	Annealing of 0.26 mm wire at 400 ^{0}C during 1 hours

Room-temperature tensile tests were conducted for as-processed bar specimens on a Zwick Z250 universal testing machine (the loading rate was 10 mm/min). The Vickers hardness (HV) was measured using a Metkon Duroline MH-6 universal tester with a load of 1 kg and a dwell time of 10 s. The hardness was measured at least five times at each point. The specific conductivity of the EMC rod and the cold rolled strip was determined using the eddy current method with a VE-26NP eddy structurescope.

The phase composition of the quaternary system Al–Zr–Fe–Si was calculated using Thermo-Calc software (TTAL5 database) [29].

3. Results

3.1. Calculation of phase composition

The element concentrations in the experimental alloy were chosen based on the following principles. According to [6,14,15,30], the concentration of zirconium corresponds to the maximum value up to which the precipitation hardening grows in an almost linear manner. The Fe and Si concentrations are close to their maximum contents in commercial aluminum and, as shown earlier [23], should ensure complete binding of iron into the Al_8Fe_2Si phase.

As can be seen from the vertical cross-section calculated at 0.4% Fe and 0.4% Si (Fig.1a), with an increase in the zirconium content the liquidus temperature rises sharply and reaches 822 °C at 0.6% Zr. This temperature corresponds to the onset of the formation of primary Al_3Zr phase crystals ($D0_{23}$), while the aluminum solid solution forms at a temperature below 660 °C. According to this cross-section, the Al_3Fe and Al_8Fe_2Si phases should also form during equilibrium solidification in addition to (Al) and Al_3Zr, the solidus temperature being 631 °C. The third iron-containing phase Al_5FeSi can only form in the solid state.

It is well-known that the non-equilibrium solidification of low-alloyed Al – Fe – Si system alloys significantly complicates their phase composition [23]. According to the calculation based on the Sheil-Gulliver model which allows one to evaluate the nature of solidification at low cooling rates, one can expect the formation of all the above mentioned iron-containing phases (see Fig.1b), as well as (Si). On the other hand, zirconium (in the amounts considered herein) at a high cooling rate can fully dissolve in (Al) [14]. There are also indications that an increased cooling rate suppresses the formation of Al_3Fe and Al_5FeSi phases in alloys containing iron and silicon at concentrations close to the selected ones [23]. Taking into account the analysis above, a corrected calculation of the non-equilibrium solidification was carried out (Fig.1c). The calculation suggests that after solidification of (Al) at 657 °C, the

Al_8Fe_2Si phase should form as part of a binary eutectic. Solidification should end at 576 °C via a eutectic reaction involving the (Si) phase, the amount of which, however, should be very small.

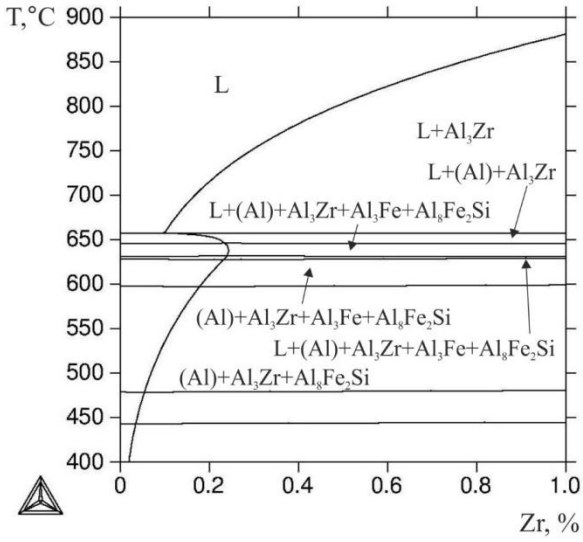

a

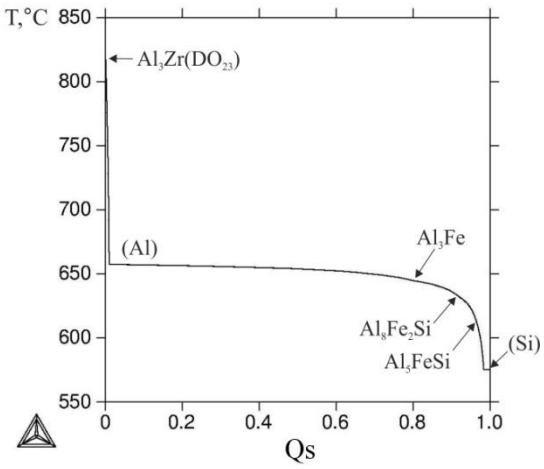

b

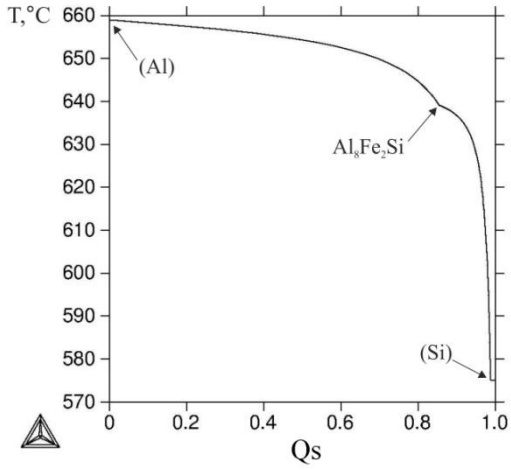

c

Figure 1. The isopleth of Al–Zr–Fe–Si phase diagram at 0.4%Fe and 0.4%Si (a) and mass fraction of solid phases (Qs) versus temperature (Sheil-Gulliver simulation) for alloy Al–0.6%Zr–0.4%Fe–0.4%Si (b,c): b) all phases are entered; c) phases Al_3Zr, Al_3Fe and Al_5FeSi are suspended (e.g. Zr in (Al))

3.2. Characterization of as-cast EMC rod

The microstructure of the as-cast billet appears to be fairly homogeneous and is characterized by a fine structure, which can be detected only by scanning electron microscopy (Fig.2a). Analysis of the microstructure did not reveal primary Al_3Zr phase crystals. This

indicates the complete dissolution of zirconium in the (Al) composition. The size of the dendritic cells is about 5 μm, which, according to [31], corresponds to a cooling rate of more than 10^3 K/s. The veins with a thickness of about 0.2 μm are revealed along the boundaries of the dendritic cells (Fig.2b). According to [32–34], such a structure is typical of the Al_8Fe_2Si phase in a small amount.

After annealing of the as-cast billet at up to 400 °C, no visible changes in the microstructure are observed. At higher temperatures, the morphology of the Fe-containing phase changes significantly. The formation of globular particles can be observed already at 450 °C (Fig.2c). It should be noted that among Fe-containing phases of the Al – Fe – Si system, only Al_8Fe_2Si is capable of spheroidization [23]. Subsequent heating to 550 °C slightly affects the microstructure (Fig.2d, e). At the maximum heating temperature (600 °C), the Fe-containing phase particles grow, the size of some particles reaching 1 μm (Fig.1f). EMPA analysis of these particles confirms their Al_8Fe_2Si composition. In addition, the particles with a size of about 0.1 μm (isolated fragment in Fig.1f), which can be interpreted as secondary precipitates of the Al_3Zr ($D0_{23}$) phase, are detected. As can be seen from the vertical cross-section shown in Fig.1a, the presence of these two phases corresponds to the equilibrium state of the considered alloy at 600 °C.

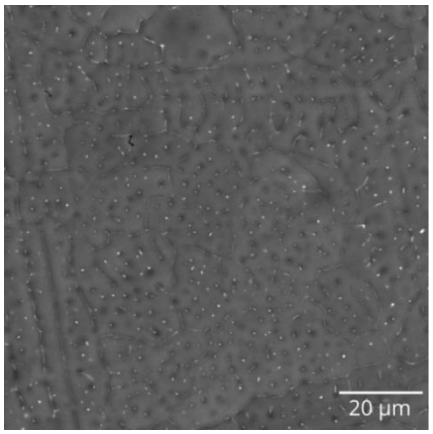

a

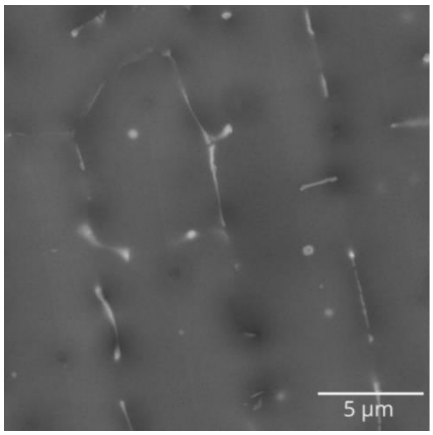

b

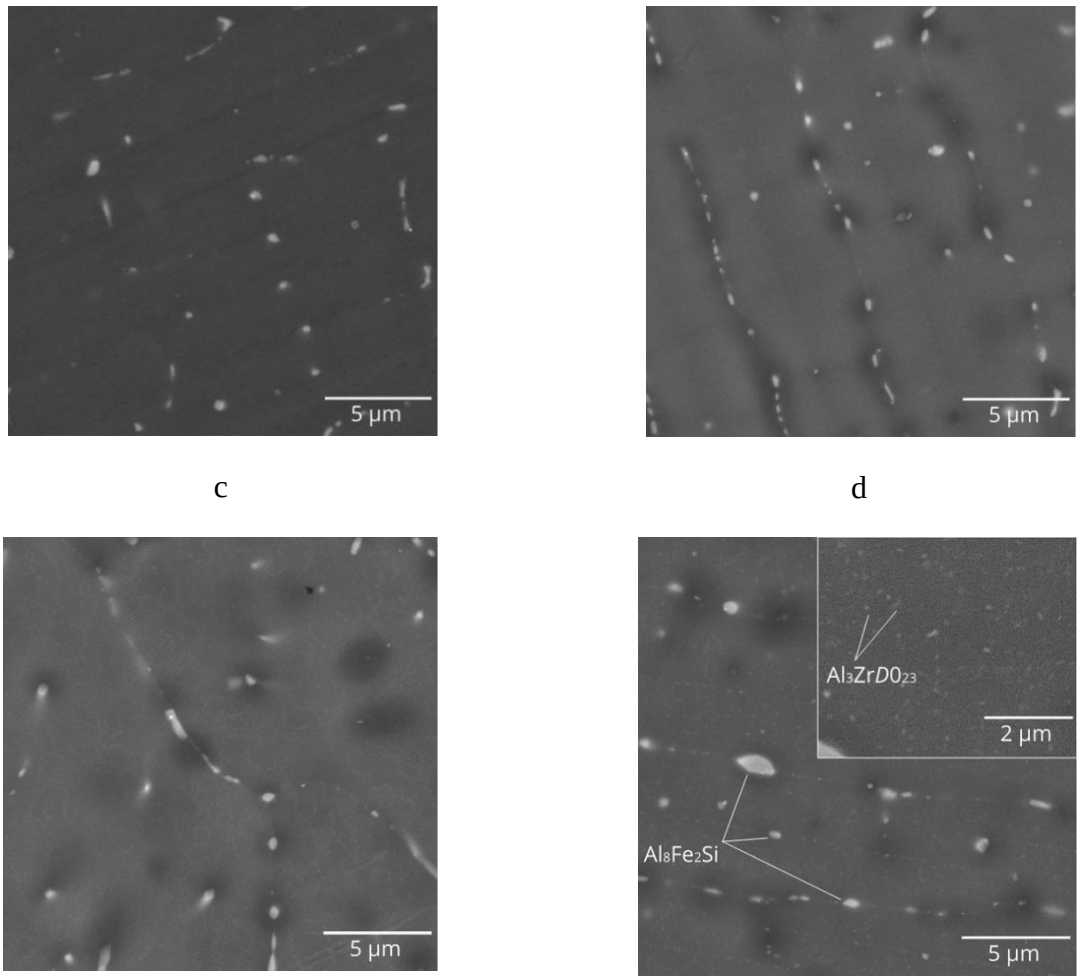

Figure 2. Effect of annealing temperature on microstructures of the Al–0.6%Zr–0.4%Fe–0.4%Si alloy, EMC rod, SEM: a,b) as-cast, c) R450, d) R500, e) R550, f) R600 (see in Table 1)

3.3. Effect of annealing and rolling on hardness and electrical conductivity

The high content of Zr in (Al) implies a significant precipitation hardening of the as-cast billet due to the formation of the $L1_2$ (Al_3Zr) phase nanoparticles. The dependence shown in Fig.3a shows that the maximum hardness which is twice the initial one (in the as-cast state) is achieved after heating at 400 °C. An increase of the annealing temperature to above 450 °C leads to softening which can be explained, primarily, by the enlargement of the Al_3Zr precipitates [9-12]. Rolling of the cylindrical billet to a 2 mm strip increases the hardness from 410 to 600 MPa, and its subsequent annealing leads to further hardening (Fig.3a). The maximal hardness of the cold rolled strip is somewhat smaller compared to that of the as-cast billet, which can be accounted for by the competition of two processes: hardening due to the formation of $L1_2$ (Al_3Zr) nanoparticles and softening due to the processes of recovery. Annealing of the strip at

higher temperatures leads to lower hardness compared to that of the EMC rod, which can be attributed to coarsening of the Al_3Zr precipitates and formation of recrystallized grains [6].

The formation of $L1_2$ (Al_3Zr) nanoparticles leads to a decrease in the Zr concentration in (Al) and, as a consequence, to an increase of the alloy electrical conductivity. The dependencies given in Fig.3b confirm this suggestion. The EC value increases from 23.8 to 31.6 MS/m for EMC rod and from 23.6 to 33.7 MS/m for cold rolled strip (i.e., by 33% and 41%, respectively). It should be noted that due to the increased density of defects in the crystal lattice, the decomposition rate of (Al) in the strip is higher [35] than that for the as-cast EMC rod. Indeed, in the former case, the maximum EC is reached after annealing at 550 ^{0}C, while in the latter case it is reached at 500 ^{0}C. In both cases, these values are higher than the maximum hardening temperature (Fig.3a). The decrease of EC at higher temperatures can be accounted for by an increase in the solubility of Zr in (Al) [6]. The EBSD analysis of the strip structure shows that the fibrous (non-recrystallized) structure formed during rolling is preserved in the as-annealed state for annealing at up to 400 °C (Fig.4a). It is clearly seen that the fibrous grains contain an extensive network of low angle boundaries. In accordance with TEM, the subgrains have an average size of about 1 μm (Fig.4b). TEM also reveals a large number of nanoparticles with a diameter of about 10 nm (Fig.4c). According to SADP (Fig.4d), these nanoparticles correspond to the $L1_2$ type phase precipitates.

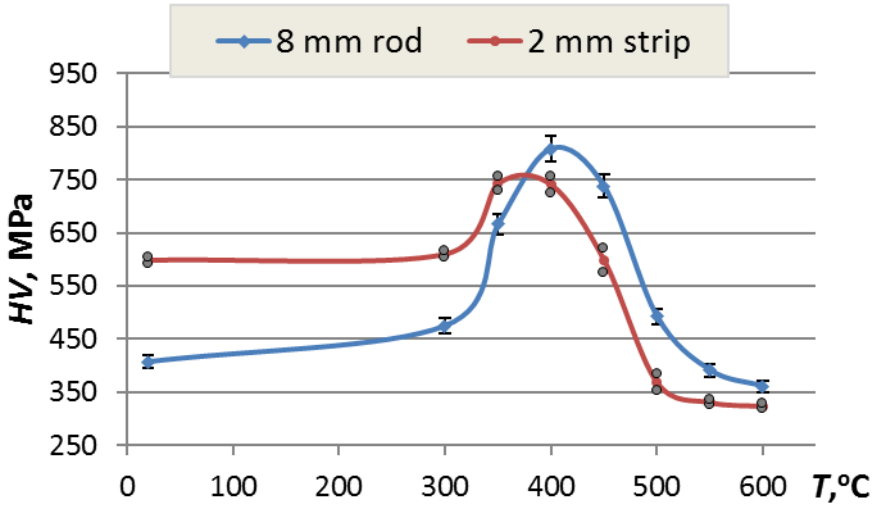

a

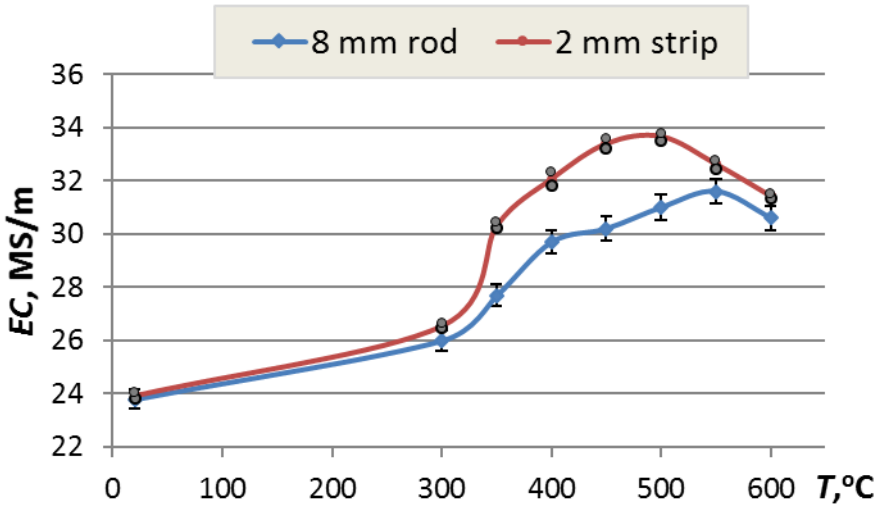

b

Fig. 3. Hardness (a) and electrical conductivity (b) vs. temperature curves for Al–0.6%Zr–0.4%Fe–0.4%Si alloy

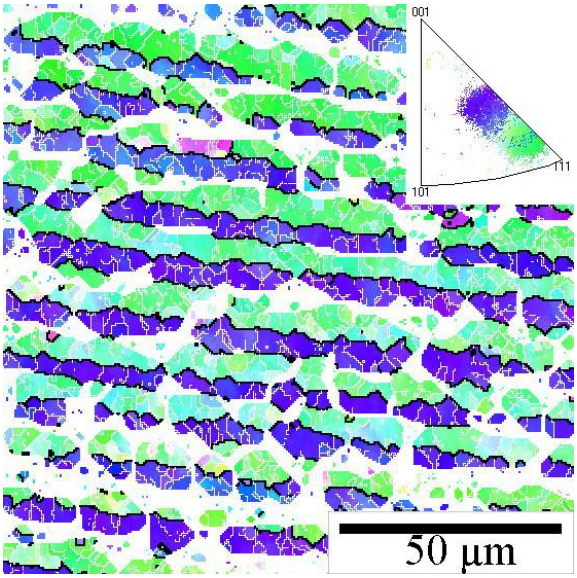

a

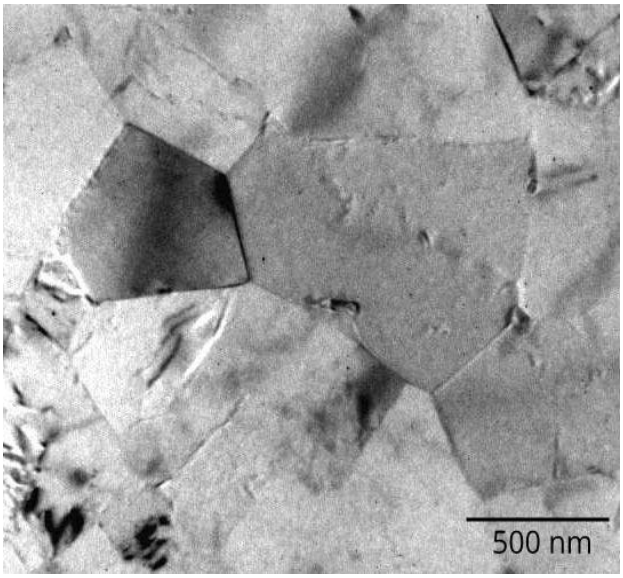

b

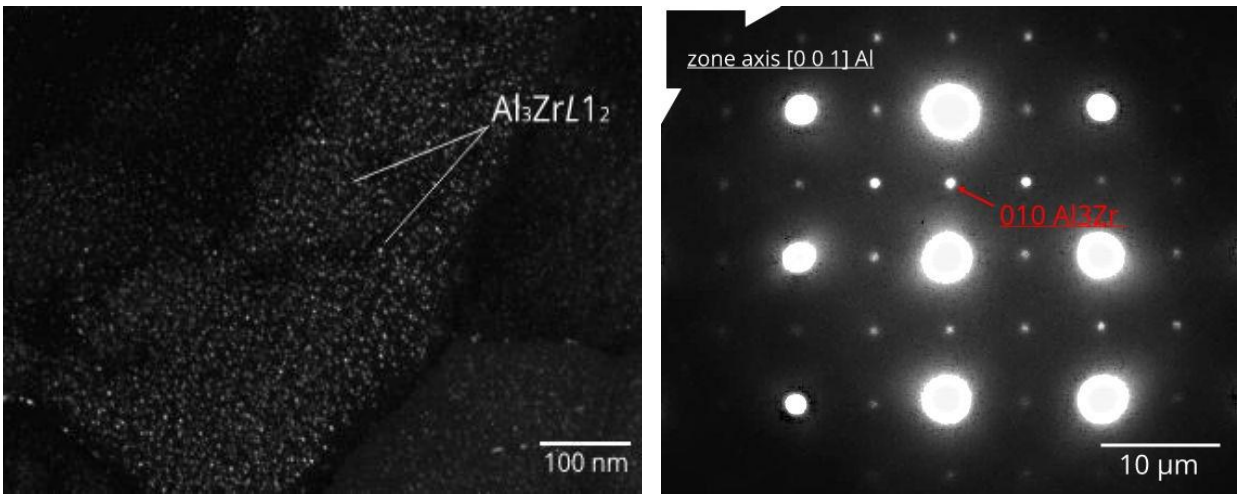

c d

Figure 4. EBSD (a) and TEM (b-d) structure of the alloy Al–0.6%Zr–0.4%Fe–0.4%Si after cold rolling and annealing at 400 ^{0}C (S400, see in Table 2): a) longitudinal direction, b) transverse direction (bright field). c) dark field, b) diffraction patterns

3.4. Properties of wire

The favorable microstructure of the as-cast EMC rod implies a high deformation plasticity, which has been experimentally confirmed during wire production using both cold rolling and drawing. As in the case of cold rolled strip, the main structural change was the formation of elongated grains, while the morphology of the Al_8Fe_2Si phase remained almost unchanged. The cold rolled wire has UTS ~ 260 MPa and YS ~ 230 MPa (zirconium must remain in (Al)). The results obtained for the strip, in particular, the temperature dependences of hardness and EC (Fig.3b) were used as the basis for choosing the annealing temperature of the wire, i.e., 400 °C. Annealing at this temperature (state W1-400) for 3 hours slightly reduced UTS and YS (Table 2). This result can be attributed to the stabilizing effect of the Al_3Zr nanoparticles. Drawing of the annealed rolled wire leads to significant strengthening. In particular, UTS are 270 MPa for the 0.5 mm wire and 300 MPa for the 0.26 mm wire. Annealing at 400 ^{0}C leads to a marked strength reduction, which, however, remains high enough for conductive alloys (UTS higher than 200 MPa).

Table 2 Mechanical properties of wires

State[1]	UTS, MPa	YS, MPa	El, %
W1	259 ± 5	233 ± 7	1.6 ± 0.4
W1-400	231 ± 4	212 ± 3	3.3 ± 0.5

W0.5	274 ± 3	259 ± 3	2.3 ± 0.2
W0.26	301 ± 5	284 ± 4	0.6 ± 0.2
W0.5-400	224 ± 6	199 ± 3	2.6 ± 0.6
W0.26-400	207 ± 3	181 ± 4	2.8 ± 0.4

[1] see in Table 2

4. Discussion

Summarizing the available information, we can conclude that the combination of strength, electrical conductivity and thermal stability in comparison with alloys containing about 0.3% Zr can be significantly improved by the addition of 0.6% Zr. This improvement can be accounted for by the formation of a favorable structure due to a combination of high solidification rate, high casting temperature, cold deformation of as-cast EMC rod and annealing of wire.

Slow cooling during solidification leads to the formation of primary Al_3Zr phase crystals ($D0_{23}$), which, due to their greater density, are sediment ~~concentrated~~ at the bottom of the ingot (Fig.5a). In addition, needle-shaped and skeletal particles whose compositions are Al_3Fe and Al_8Fe_2Si, respectively, are detected in the structure of the slowly cooled sample. These changes correspond to the simulation of non-equilibrium crystallization shown in Fig.1b. The microstructure of the sample obtained by water quenching of the initial billet after 1 hour exposure at 750^0C (i.e. melt production) also reveals the presence of the primary Al_3Zr phase crystals (Fig.5b). This is because this temperature is below the liquidus temperature of the alloy (see in Fig.1a). Thus the combination of high temperature of melt and rapid solidification achieved in the EMC method leads to the desired microstructure of the as-cast rod (Fig. 2a,b). For comparison, Fig. 1 shows the microstructure of the alloy obtained during solidification in a graphite mold (with a size of 10 x 40 x 200 mm). Due to the relatively low cooling rate (~10 K/s), which is typical of industrial production [23], the alloy structure contains a small amount of unacceptable primary Al_3Zr phase crystals.

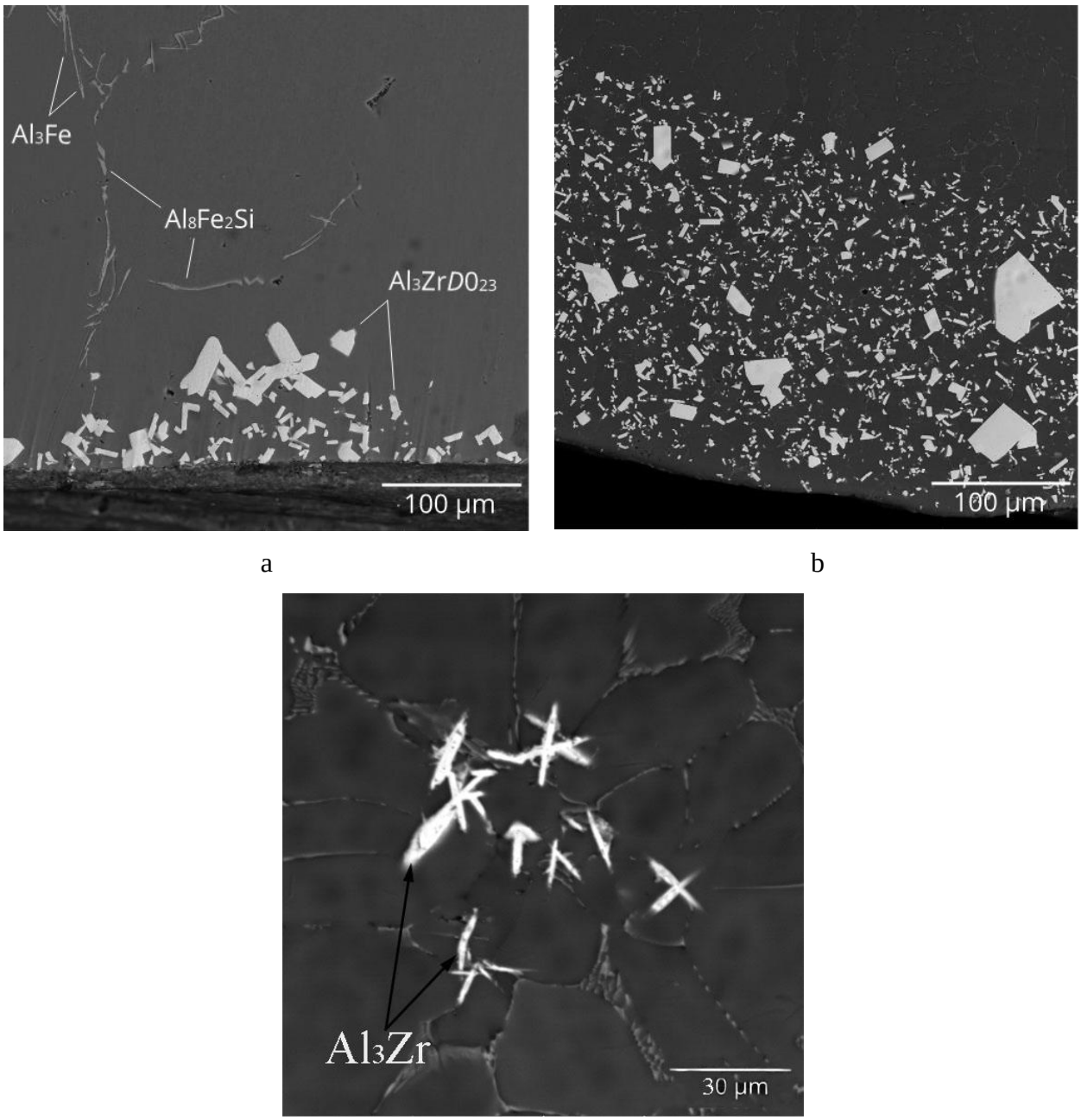

Figure 5. Microstructures of the alloy Al–0.6%Zr–0.4%Fe–0.4%Si after slow cooling from 850 ^{0}C (a), after quenching from 750 ^{0}C (b) and after solidification in a graphite mold (cooling rate is about 10 K/s). SEM:

The dependencies of the hardness versus annealing temperature shown in Fig.3a allow us to estimate the potential hardening and thermal stability. Since heating at 400 °C corresponds to the maximum hardness, it is obvious that the wire should be annealed at this temperature. Such annealing stabilizes the structure at the maximum operating temperatures of the conductor alloys (according to IEC 62004: 2007). Thus, unlike the CCR technology which includes continuous annealing of wire [7,8], the EMC technology provides a significant reduction of the production cycle.

The desired combination of strength, ductility and electrical conductivity (EC) can be achieved by selecting the chemical composition and annealing mode. Since any alloying that is required for achieving strength and, especially, thermal stability leads to a decrease in the electrical conductivity, it is advisable to estimate the maximum achievable EC. In the case of Al – Zr – Fe – Si alloys, the maximum EC level can be approximately calculated using the equation:

$$EC=(Q / 100) \cdot (EC_0 - C_{Zr} \cdot K_{Zr} - C_{Si} \cdot K_{Si}) \quad (1)$$

where Q is the fraction of (Al) (wt.%), EC_0 is the electrical conductivity of pure aluminum (MS/m), C_{Zr} and C_{Si} are the concentrations of Zr and Si in (Al) (wt.%), and K_{Zr} and K_{Si} are the coefficients of Zr and Si on EC (per 1 wt.%)

From earlier work [26] where the separate and joint influence of zirconium and silicon on the properties of pure aluminum was considered it follows that the coefficients K_{Zr} and K_{Si} are ~ 20 and ~ 10, respectively. To estimate EC using Eq. (1), it is also necessary to determine Q, C_{Zr} and C_{Si}. For this purpose, we calculated the phase composition of the alloy for the case of the iron is completely bound into the Al_8Fe_2Si phase. The calculated EC values were compared with experimental data for the strip (see in Fig.3b). As can be seen from Table 3, at 450 ^{0}C there is a good match between the calculated and the experimental values. This suggests that the proposed equation is adequate. On the other hand, at 400 ^{0}C the calculated EC is higher than the experimental one. This can be attributed to the fact that the annealing time was insufficient to achieve the equilibrium solubility of Zr in (Al). With decreasing temperature, the diffusion rate of zirconium in (Al) decreases and thus it requires longer exposures which can be hundreds of hours [7, 8]. Therefore, annealing the wire at temperatures below 400 °C seems impractical, despite the potential to achieve higher EC values.

Table 3 Calculated phase composition and electrical conductivity (EC) for some alloys of Al–Zr–Fe–Si system

T, ^{0}C	Fractions of phases, wt.%				Concentrations in (Al), wt.%			EC, MS/m (IACS)	
	Al_8Fe_2Si	(Si)	Al_3Zr	(Al)	Si	Fe	Zr	Calc	Exper
Al–0.6%Zr–0.4%Fe–0.4%Si									
400	1.23	0.04	1.10	97.64	0.26	<0.01	0.02	34.0 (58.6)	32.1 (55.3)
450	1.22	–	1.10	97.72	0.30	<0.01	0.04	33.2 (57.2)	33.4 (57.0)
Al–0.6%Zr–0.4%Fe–0.15%Si									

400	1.22	–	1.10	97.68	0.05	<0.01	0.02	36.0 (62.1)	–
Reference alloy Al–0.28%Zr–0.14%Fe–0.07%Si [6]									
400	0.41	–	0,46	99.13	0.02	<0.01	0.02	36.4 (62,8)	33.4 (57.6)
Al–0.6%Zr–1.2%Fe–0.4%Si									
400	3.68	–	1.10	95.22	0.09	<0.01	0.02	34.8 (60.0)	–

Since it is impossible to reduce the residual solubility of Zr in (Al), it is advisable to consider the possibility of reducing the concentration of Si in (Al) in order to increase the EC. As can be seen from Table 3, the reduction of silicon content in the alloy to 0.15 % makes it possible to reduce its concentration in (Al) to 0.05%, which implies an increase in EC up to 36.0 (almost to the level of the reference alloy Al – 0.28% Zr – 0.14% Fe– 0.07% Si). The concentration of Si in (Al) can be reduced by increasing the iron content due to the formation of the Al_8Fe_2Si compound. For instance, the addition of 0.8% Fe into the experimental alloy (i.e., up to 1.2%) according to the calculation suggests an increase in the EC from 34.0 to 34.8 MS/m, although the amount of the Al_8Fe_2Si phase increases by 3 times. This is due to the fact that the effect of reducing the concentration of Si in (Al) (from 0.26 to 0.09%) is more significant than the decrease of the fraction of (Al).

Thus, the use of the EMC technology for the Al-Zr-Fe-Si system alloys provides several advantages. First, this is an increase in the zirconium content in (Al) compared to the CCR technology, which allows increasing the strength and maximum operating temperature. Secondly, excluding the hot rolling operation from the wire production process simplifies the technology (up to combining continuous casting with drawing). Thirdly, the fine microstructure (submicron size of eutectic particles) allows increasing the permissible contents of iron and silicon, which implies economic advantages.

5. Conclusions

1. For the experimental Al – 0.6% Zr – 0.4% Fe – 0.4% Si alloy, it was shown that, due to the high cooling rate during solidification, the method of electromagnetic casting (EMC) shows good promise for obtaining wires with an improved combination of strength, electrical conductivity and thermal stability.

2. Using both experimental and computational methods, it was shown that in order to ensure complete dissolution of zirconium into an aluminum solid solution, the casting temperature should be above 820 ° C.

3. The iron in the as-cast billet is fully included in the Al_8Fe_2Si phase, which has the form of veinlets located along the boundaries of the dendritic cells. Annealing at above 400 °C leads to the formation of globular particles of this phase.

4. The cast billet obtained by the EMC method has a high ductility during cold deformation, which allows drawing a wire with high degrees of deformation (more than 98%).

5. It is shown that 400–450 °C annealing of a cold-rolled strip obtained from a cast billet allows increasing both the electrical conductivity and the hardness. This is due to the formation of Al_3Zr ($L1_2$) phase nanoparticles and, as a result, a decrease of the zirconium concentration in the aluminum solid solution.

~~6. The ability to electromagnetically cast wire rod that could be cold deformed directly (without hot rolling) would be a substantial economic advantage.~~

Acknowledgements

The study was carried out within the framework of the implementation of the Resolution of the Government of the Russian Federation of April 9, 2010 No. 220 (Contract No. 074-02-2018-329 from May 16, 2018).

REFERENCES

1. ASTM B941-16, Standard specification for Heat Resistant Aluminum-Zirconium Alloy Wire for Electrical Purposes, ASTM International, West Conshohocken, PA, 2016.
2. J.P. Brubak, B. Eftestol, F. Ladiszlaidesz, «Aluminium alloy, a method of making it and an application of the alloy» (IFI CLAIMS Patent Services, 2019), https://patents.google.com/patent/US5067994A/en?oq=5067994. Accessed 30 April 2019.
3. T. Knych, M. Jablonsky, B. Smyrak, *Arch. Metall. Mater*, 54, 671 (2009).
4. I. Properzi, «Machine for the continuous casting of metal rods», (IFI CLAIMS Patent Services, 2019), https://patents.google.com/patent/US2659949A/en?oq=2659949. Accessed 30 April 2019.
5. Information on https://www.southwire.com. Accessed 30 April 2019.
6. N.A. Belov, A.N. Alabin, I.A. Matveeva, D.G. Eskin, *Trans. Nonferrous Met. Soc. China* (2015) doi: 10.1016/S1003-6326(15)63907-3.

7. E. Çadırlı, H. Tecer, M. Sahin, E. Yimaz, T. Kirindi, M. Gündüz, *J. Alloys Compd.* (2015) doi: 10.1016/j.jallcom.2015.01.193.
8. J.D. Robson, P.B. Prangnell, *Acta Mater.* (2001) doi: 10.1016/S1359-6454(00)00351-7.
9. K.E. Knipling, R.A. Karnesky, C.P. Lee, D.C. Dunand, D.N. Seidman, *Acta Mater.* (2010) doi: 10.1016/j.actamat.2010.05.054.
10. A. Deschamp, P. Guyo, *Acta Mater.* (2007) doi: 10.1016/j.actamat.2006.12.015.
11. W. Lefebvre, F. Danoix, H. Hallem, B. Forbord, A. Bostel, K. Marthinsen, *J. Alloys Compd.* (2009) doi: 10.1016/j.jallcom.2008.02.043.
12. B. Forbord, W. Lefebvre, F. Danoix, H. Hallem , K. Marthinsen, *Scripta Mater.* (2004) doi: 10.1016/j.scriptamat.2004.03.033.
13. E. Clouet, A. Barbu, L. Lae, G. Martin, *Acta Mater*, 53, 2313 (2005).
14. N.A. Belov, A.N. Alabin, D.G. Eskin, and V.V. Istomin-Kastrovskiy, *J. Mater. Sci.* (2006) doi: 10.1007/s10853-006-0265-7.
15. N.A. Belov, A.N. Alabin, A.A. Yakovlev, *Izv. Vuzov. Tsvet. Metall. (Proc. Higher Schools Nonferr. Metal)*. (2013) doi: 10.17073/0021-3438-2013-2-50-55.
16. J.W. Evans, *JOM*, 47, Is. 5, 38 (1995).
17. A.A. Avdulov, G.P. Usynina, N.V. Sergeev, I.S. Gudkov, *Tsvet. Met*. (2017) doi: 10.17580/tsm.2017.07.12.
18. V.I. Dobatkin, V.I. Elagin, V.M. Fedorov. *Bystrozakristallizovannye alyuminievye splavy (Rapidly Solidified Aluminum Alloys)*, (Moscow, M: VILS, 1995), pp. 43-59.
19. S.I. Berman. *Proizvodstvo granul iz splavov na osnove alyuminiya i pressovanie iz nih polufabrikatov (Production of granules from aluminum-based alloys and pressing of semi-finished products)*, (Moscow, M: Cvetmetinformaciya, 1971), pp. 101
20. I.J. Polmear, *Light Metals: From Traditional Alloys to Nanocrystals*, 4th ed. (Oxford, UK: Elsevier, 2006), pp. 188-193.
21. G. Zeer, M.V. Pervukhin, E.G. Zelenkova, *Met. Sci. Heat Treat.* (2011) doi: 10.1007/s11041-011-9370-6.
22. N.A. Belov, D.G. Eskin, A.A. Aksenov, *Multicomponent phase diagrams: applications for commercial aluminum alloys*, (Amsterdam, NL: Elsevier, 2005), pp. 19-31.
23. M.V. Glazoff, A.V. Khvan, V.S. Zolotorevsky, N.A. Belov, Alan T. Dinsdale, *Casting Aluminum Alloys. Their Physical and Mechanical Metallurgy.* (Oxford, UK: Elsevier, 2019), pp. 180-186.
24. J.E. Hatch, ed., *Aluminum—Properties and Physical Metallurgy* (Metals Park, OH: ASM, 1984), pp. 59-64.

25. C. Booth-Morrison, Z. Mao, M. Diaz, D.C. Dunand, C. Wolwerton, D.N. Seidman, *Acta Mater*. (2012) doi: 10.1016/j.actamat.2012.05.036.
26. N.A. Belov, N.O. Korotkova, A.N. Alabin, S. S. Mishurov, *Russ. J. Non-ferrous Metals.* (2018) doi: 10.3103/S1067821218030033.
27. T. Gao, A. Ceguerra, A. Breen, X. Liu, Yu. Wu, S. Ringer, *J. Alloys Comd*. (2016) doi: 10.1016/j.jallcom.2016.02.236.
28. Information on http://www.npcmgd.com. Accessed 25 April 2019
29. Information on www.thermocalc.com. Accessed 30 March 2019
30. N.A. Belov, A.N. Alabin, A.Yu. Prokhorov, *Russ. J. Non-ferrous Metals.* (2009) doi: 10.3103/S1067821209040099.
31. L. Bäckerud, G. Chai, J. Tamminen. *Solidification Characteristics of Aluminum Alloys. Vol. 1: Foundry Alloys*, (Oslo, NO: Skanaluminium, 1986), pp. 9-26.
32. N.A. Belov, A.A. Aksenov, D.G. Eskin, *Iron in aluminum alloys: impurity and alloying element*, (London, UK: Fransis and Tailor, 2002). 360 p.
33. A. Školáková, P. Novák, D. Vojtěch, T.F. Kubatík, *Mater. Des.* (2016) doi: 10.1016/j.matdes.2016.06.069.
34. H. Chen, Q. Chen, Y. Du, J. Brataberg, A. Engstrom, Update of Al−Fe−Si, Al−Mn−Si and Al−Fe−Mn−Si thermodynamic descriptions [J]. Trans. Nonferrous Met. Soc. China (2014) doi: 10.1016/S1003-6326(14)63310-0.
35. Y.Nasedkina, X. Sauvage, E.V. Bobruk, M. Yu. Murashkin, R.Z. Valiev, N.A. Enikeev, *J. Alloys Comd*. (2017) doi: 10.1016/j.jallcom.2017.03.312 0925-8388